THE SEARCH FOR "JENYON'S CHANNEL": THE MISSING LINK BETWEEN THE PERMIAN BASINS IN THE NORTH SEA.

Thomas D. Houghton, Rachel E. Brackenridge, Joyce E. Neilson, John R. Underhill.

Corresponding Author: Thomas D. Houghton

Thomas D. Houghton: t.houghton.22@abdn.ac.uk

Rachel E. Brackenridge: rachel.brackenridge@abdn.ac.uk

Joyce E. Neilson: j.neilson@abdn.ac.uk

John R. Underhill: john.underhill@abdn.ac.uk

Address: Centre for Energy Transition, School of Geosciences, University of Aberdeen, Meston Building, King's College, Aberdeen, United Kingdom, AB24 3UE

ABSTRACT

The Mid North Sea High (MNSH) Seaway, otherwise known as Jenyon's Channel, was the only major marine connection between the Northern and Southern Zechstein Basins during the latest Permian. Current understanding favours a model where marine replenishment began with a northern connection to the Panthalassic Ocean (along a network of basins that were precursors to the North Atlantic Rift System), after which marine water passed into the Northern Zechstein Basin, travelled through the MNSH Seaway before finally reaching the Southern Zechstein Basin. This study delineates evaporite formations in an extensive petrophysical dataset to analyse marine connections and whether they influenced Zechstein facies distribution. The first four Zechstein Cycles (Z1-Z4) are identified on the MNSH platform which shows that this structure was always covered by a thin water column during sea-level highstand; however, during Z2 sea-level lowstand, the MNSH

Seaway provided the main connection between the basins. As relative sea-level fell, the MNSH Seaway became increasingly constricted resulting in hypersalinity due to limited volumes of marine water reaching the Southern Zechstein Basin. This system precipitated vast volumes of Z2 (late Wuchiapingian) halite in the Southern Zechstein Basin, whereas this facies remains reduced in the Northern Zechstein Basin. In Z3 and Z4 (Changhsingian) times relative average sea-level was higher resulting in sustained communication between the basins, even in times of sea-level lowstand. This is evidenced through a regionally traceable blanket of Z3 halite, along with occasional examples of Z2 carbonate platforms becoming entombed in Z3 halite. This work provides revised palaeoenvironmental understanding for the latest Permian. The workflow could also aid in the study of other oceanic gateways with further implications for hydrocarbon exploration efforts and emerging energy transition technologies such as subsurface storage on the UK Continental Shelf.

KEY WORDS

Mid North Sea High.

Zechstein.

Seaway.

Petrophysics.

Basin connectivity.

Restricted basins.

1. INTRODUCTION

The Mid North Sea High (MNSH) is a major east-west striking elevated palaeotopographical feature which separated the Northern and Southern Zechstein Basins during the latest Permian. The structure traverses the UK sector of the North Sea before joining with the Ringkøbing Fyn High in the east. Whilst once perceived as an unimpeded barrier, a north-south trending channel through the MNSH has been postulated but largely undocumented for almost 50 years (Ziegler, 1975; Day et al., 1981). Despite this, poor seismic data coverage and a general structural alignment with the Central Graben resulted in interpretations of the channel as a Mesozoic half-graben. Jenyon et al. (1984) had access to the first seismic dataset with sufficiently closely spaced lines to provide an updated assessment of the channel. Their analysis identified salt dissolution structures and salt slopes alongside a uniform base Zechstein reflector, the contrast between which allowed for the feature to be reinterpreted as a pre-Mesozoic channel with primary salt precipitation geometry. Accordingly, subsequent studies progressed based on the interpretation of the channel as a connection between basins (Jenyon, 1987; Jenyon and Taylor, 1988; Smith and Taylor, 1989). Although a lack of well coverage and modern seismic data within the seaway lead to a perceived lack of prospectivity which inhibited further investigation, the acquisition of new densely spaced 2D and 3D seismic data now allows for a reinvestigation of this feature. Straits and seaways connect basins, control the exchange of water, heat, biota, and sediments, and can also influence regional climate systems (Rossi, 2023). As such, uncovering the periods of time when the seaway exerted influence will be key for understanding the spatial and temporal evolution of the Zechstein system.

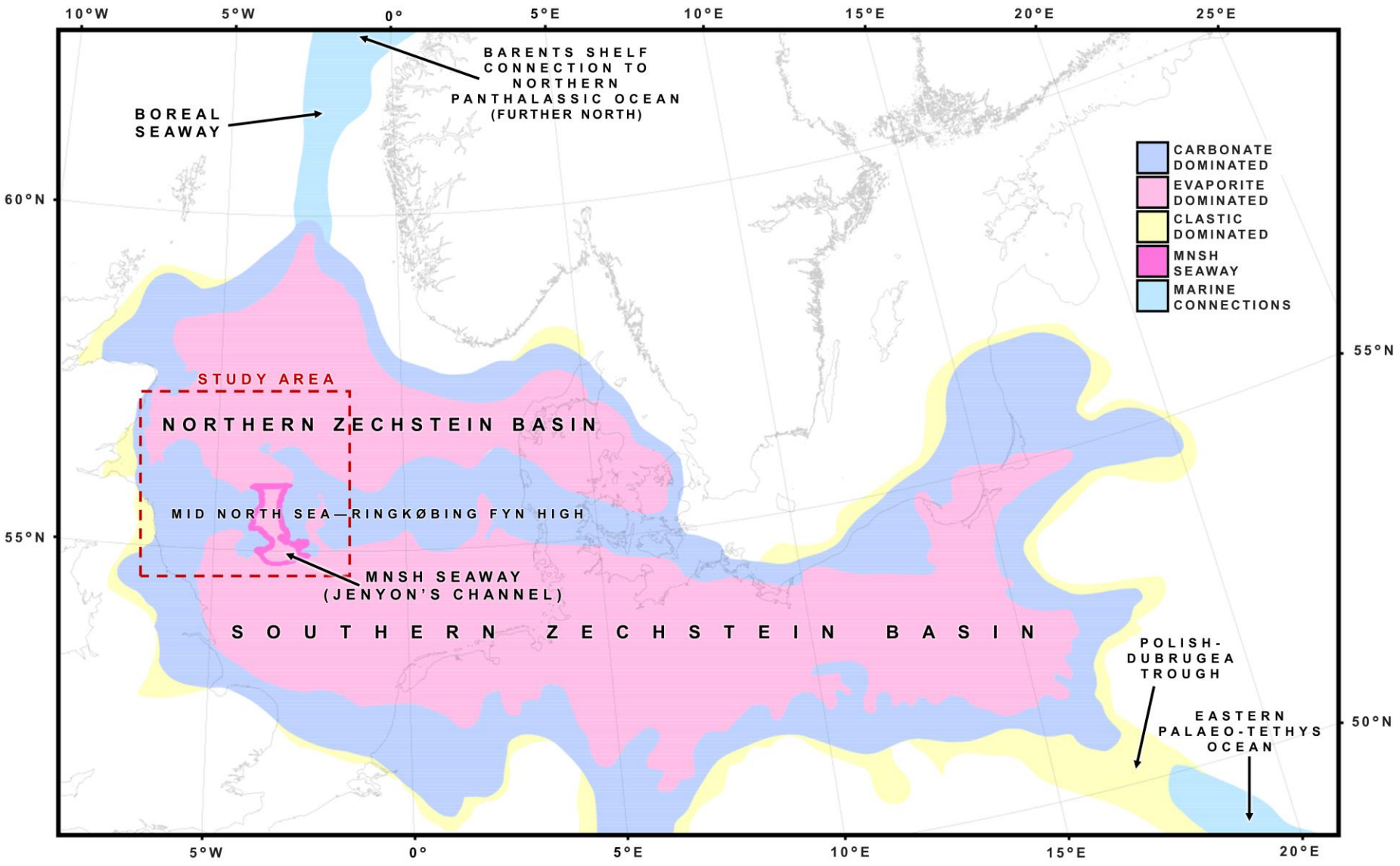
10°W
5°W
0°
5°E
10°E
15°E
20°E
25°E
60°N
55°N
50°N
BARENTS SHELF CONNECTION TO NORTHERN PANTHALASSIC OCEAN (FURTHER NORTH)
BOREAL SEAWAY
CARBONATE DOMINATED
EVAPORITE DOMINATED
CLASTIC DOMINATED
MNSH SEAWAY
MARINE CONNECTIONS
STUDY AREA
NORTHERN ZECHSTEIN BASIN
MID NORTH SEA—RINGKØBING FYN HIGH
MNSH SEAWAY (JENYON'S CHANNEL)
SOUTHERN ZECHSTEIN BASIN
POLISH-DUBRUGEA TROUGH
EASTERN PALAEO-TETHYS OCEAN

Fig. 1. *Regional facies distribution during Zechstein deposition after Ziegler (1988), with improvements to the MNSH after Brackenridge et al. (2020).*

Brackenridge et al. (2020) used regional 2D seismic data to understand the stratigraphic evolution of the MNSH, and their Zechstein mapping defined the lateral trends of the seaway at a higher resolution than that of Jenyon et al. (1984). Despite the improved mapping of the MNSH Seaway, this research did not examine the impact on Zechstein facies across the study area. The Zechstein system on the UK Continental Shelf is emerging as a key target not only for hydrocarbon exploration (Patruno et al., 2017; Grant et al., 2019; Brackenridge et al., 2020; Browning-Stamp et al., 2023; Garland et al., 2023), but also for subsurface storage in solution-mined halite caverns (Muhammed et al., 2022; Marín et al., 2023; Brackenridge et al., 2023).

This study aims to build on recent seismic mapping (Brackenridge et al., 2020; Browning-Stamp et al., 2023; Garland et al., 2023) to constrain the times of seaway influence and how implications vary for the Northern and Southern Zechstein Basins. This has been achieved through a re-evaluation of petrophysical data from legacy exploration wells to construct a series of well correlation panels across the western region of the Northern Zechstein Basin and the northwesternmost part of the Southern Zechstein Basin, as these regions flank the MNSH Seaway (fig. 1). Further well correlation panels will be used to understand key localities that help decipher the implications of the MNSH Seaway. Ultimately, this study provides evidence that petrophysical data can help reveal the existence and reconstruct the evolution of a major marine gateway between two semi-restricted basins without the need for extensive 3D seismic coverage.

2. GEOLOGICAL SETTING

During the late Palaeozoic, the Variscan Orogeny amalgamated the Gondwana, Laurussia and Siberia landmasses to form the Pangea Supercontinent. This set the scene for the future development of the Zechstein Sea in the late Permian (Glennie and Underhill, 1998; McCann et al., 2006; Fluteau et al., 2001; Kroner and Romer, 2013; Schulmann et al., 2014; Underhill and Richardson, 2022). The surface of Pangea consisted of intracontinental regions of terrestrial dryland within which developed the early-middle Permian Rotliegend desert red beds (McKie, 2017; Underhill and Richardson, 2022). The Permo-Triassic boundary marks a tectonic shift from dominant continental accretion in the Palaeozoic to major Mesozoic rifting which eventually resulted in the breakup of Pangea (Coward, 1995).

A minor phase of rifting during the early Permian not only closed the Rheic Ocean (which lay between Laurentia and Gondwana) but also developed two new Permian intracratonic basins partitioned by the Mid North Sea - Ringkøbing Fyn High (Jenyon and Taylor, 1988; Heeremans et al., 2004; McCann et al., 2006; Nance et al., 2009, 2011; Mulholland, 2018; Brackenridge et al., 2022; Underhill and Richardson, 2022). Defined as a palaeotopographical high of lower Palaeozoic strata with a Caledonian granite core, this system was generated in association with Permian rifting, which subsequently caused the thinning of Rotliegend and Zechstein stratigraphy (Donato et al., 1983; Corfield et al., 1996; Patruno et al, 2017; Grant et al., 2020). The Northern Zechstein Basin is the more laterally restricted of the two basins, whilst the Southern Zechstein Basin extends across Germany, Poland, the Netherlands, Denmark, and the United Kingdom (Doornenbal and Stevenson, 2010, Underhill and Richardson, 2022). The Southern Zechstein Basin sits on deformed and tilted Carboniferous and Devonian strata which

were once part of the foreland of the Variscan thrust belt (Ziegler 1992, Grant et al., 2019).

The Zechstein basin system was originally infilled by Rotliegend desert sediments; however, in the latest Permian marine waters from the northern reaches of the Panthalassic Ocean transgressed along an incipient arm of the proto-North Atlantic Rift System. This produced the Boreal Seaway connection between the Northern Zechstein Basin and the Barents Shelf of the Panthalassic Ocean (Ziegler, 1988; Sørensen et al., 2007; Underhill et al., 2023; fig. 1). This transgression via the new marine connection initiated the Zechstein Sea since the Permian basin system was flooded with cooler northern marine waters.

Whilst the southeastern Polish-Dubrugea Trough connected the Southern Zechstein Basin and the Eastern Palaeo-Tethys Ocean until the Early Permian, this connection was limited or interrupted in the Middle and Late Permian (Sørensen et al., 2007; McKie, 2017). Deposition in Zechstein times across the Polish-Dubrugea Trough mainly exhibits deltaic/shallow marine sands (Ziegler, 1988). In contrast, the Boreal Seaway features carbonates and evaporites, which could suggest that the northern connection was characteristically akin to the Zechstein Sea. Palaeontological studies of bryozoa have confirmed that the Zechstein basin system was mainly replenished by cooler northern marine waters (Sørensen et al., 2007; Patruno et al., 2022), and therefore palaeoenvironmental studies use a model where the Boreal Seaway was the main influence on the Zechstein Sea even in a scenario where global highstand allowed for sporadic connection to the Eastern Palaeo-Tethys Ocean via the Polish-Dubrugea Trough (fig. 1).

The Zechstein Sea was only intermittently connected to the Panthalassic Ocean which resulted in cyclical variations in basin salinity (Tucker, 1991). As

such, the fauna of the Zechstein Sea differ from those in the broader Permian biostratigraphic scheme. The Zechstein Supergroup (fig. 2) is a pan-northwest European unit which can be broadly divided into 5 depositional sequences of carbonates and evaporites attributed to repeated flooding and evaporation corresponding to cyclical variations in salinity (Clark, 1986; Smith, 1979; Tucker, 1991; Jackson and Stewart, 2017; Fig. 2). The Z2 Stassfurt Halite Fm., the Z3 Leine Halite Fm., and the Z4 Aller Halite Fm. are the key units studied in this research (emphasised in fig. 2).

The lateral extent of Pangea allowed for significant aridity which amplified global greenhouse conditions (Habicht, 1979; Glennie, 1995; Peryt et al., 2012; Grant et al., 2017; McKie, 2017). The polar regions of the globe remained mostly free of ice, signifying a period of global highstand. The late Permian saw Northern Panthalassic marine waters transgress over 1000km, eventually reaching as far as the East Irish Sea, the Netherlands, and Poland. This suggests that the floors of the Permian basins were below global sea-level (McKie, 2017). Average sea-level trends for the late Permian and Triassic remain poorly constrained; nonetheless, in general, studies observe long-term sea-level rise (McKie, 2017).

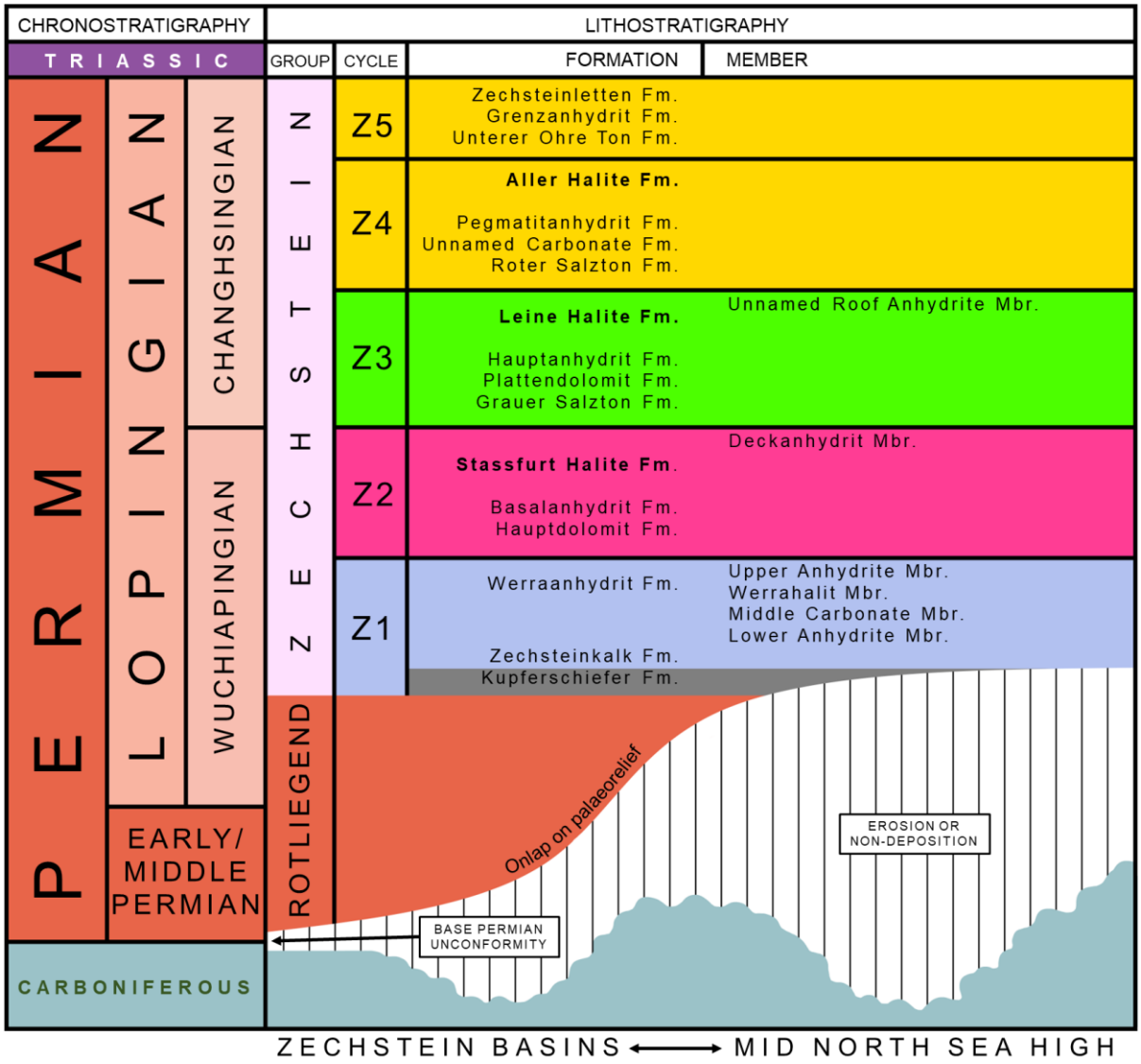

Fig. 2. *Stratigraphy of the Zechstein around the MNSH after the Southern North Sea classification provided by Johnson et al. (1994) and Grant et al. (2019). The colours allocated to Zechstein subdivisions remain consistent throughout this study.*

3. DATA AND METHODOLOGY

The petrophysical data used in this study cover the greater MNSH region (Quadrants 20-21, 26-30, 36-44) and were acquired from the North Sea Transition Authority National Data Repository (fig. 3b). At first, 120 wells were

identified which, at minimum, penetrated the top of the Zechstein. As comparisons between evaporite thicknesses were important to this study, the focus moved to 50 wells which penetrate the complete Zechstein interval. Across the Southern Zechstein Basin, the sheer abundance of exploration allowed for the study to proceed with high-grade wells with complete suites of petrophysical logs. In contrast, a lack of legacy exploration data within the MNSH Seaway and Northern Zechstein Basin prompted the use of some wells with slightly limited data availability (table 1); however, in such cases, interpretation was controlled and calibrated using analogues from high-confidence neighbouring wells. Wireline logs were used to diagnose different lithologies (Rider, 1996; SaltWorksConsultants, 2023; summarised in table 2). These responses were mapped to formations and members from the Southern North Sea classification of the Zechstein (fig. 2) from which changes in package thicknesses could be monitored across the study area. Well tops corresponding to every formation and member were created across 50 wells. This paper presents findings from 23 representative wells which are organised into a series of five well correlation panels (fig. 4).

a)

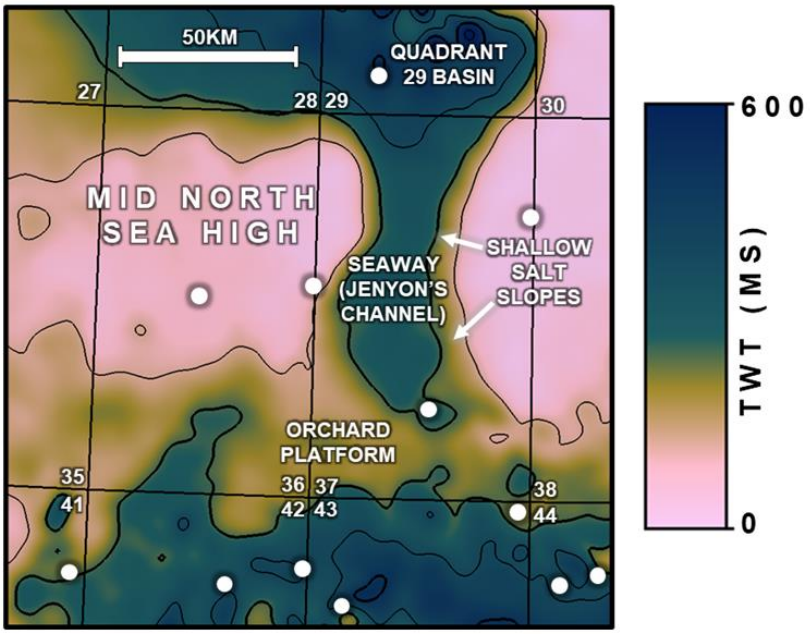
50KM
QUADRANT
29 BASIN
27
28 29
30
MID NORTH
SEA HIGH
SEAWAY
(JENYON'S
CHANNEL)
SHALLOW
SALT
SLOPES
ORCHARD
PLATFORM
35
41
36 37
42 43
38
44
600
TWT (MS)
0

b)

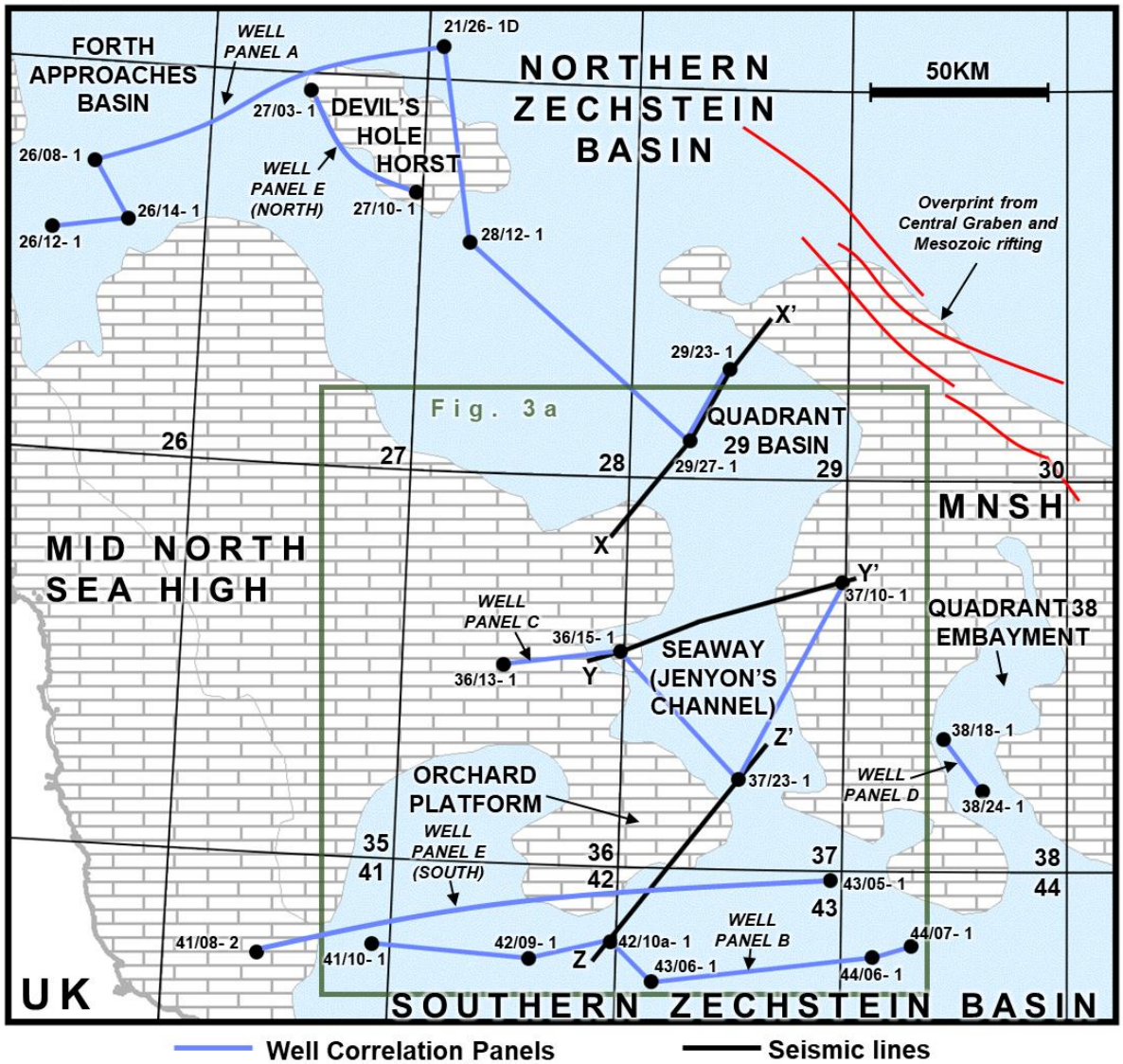
FORTH
APPROACHES
BASIN
WELL
PANEL A
21/26- 1D
NORTHERN
ZECHSTEIN
BASIN
50KM
27/03- 1
DEVIL'S
HOLE
HORST
26/08- 1
WELL
PANEL E
(NORTH)
27/10- 1
26/14- 1
26/12- 1
28/12- 1
Overprint from
Central Graben and
Mesozoic rifting
X'
29/23- 1
Fig. 3a
QUADRANT
29 BASIN
29/27- 1
26
27
28
29
30
X
MNSH
MID NORTH
SEA HIGH
Y'
37/10- 1
WELL
PANEL C
36/15- 1
36/13- 1
Y
SEAWAY
(JENYON'S
CHANNEL)
QUADRANT 38
EMBAYMENT
38/18- 1
Z'
37/23- 1
WELL
PANEL D
38/24- 1
ORCHARD
PLATFORM
WELL
PANEL E
(SOUTH)
35
41
36
42
37
43
38
44
43/05- 1
41/08- 2
41/10- 1
42/09- 1
Z
42/10a- 1
WELL
PANEL B
43/06- 1
44/07- 1
44/06- 1
UK
SOUTHERN ZECHSTEIN BASIN
Well Correlation Panels
Seismic lines

Fig. 3. *The MNSH Study area* ***a)*** *Zechstein two-way-time thickness map created using surfaces available on the NSTA Data Centre (Brackenridge et al., 2018) showing the seismically derived ground truth behind the interpretation of the MNSH Seaway. The map shows lateral continuity of the shallow salt slopes first identified by Jenyon et al. (1984) which allowed for the reinterpretation of the feature as a seaway. The location of this map and well IDs can be found in fig. 3b* ***b)*** *Map of the data used in this study and the position of well correlation panels and seismic lines (map after Brackenridge et al., 2020)*

The neutron-density (NPHI-RHOB) logs were plotted on the scales of 45 to -15 cm^3/cm^3 and 1.95 to 2.95 g/cm^3 respectively. As a result, when the logs track each other, it is an indication that the lithology could be limestone; however, most carbonates within the study area are dolomitised (that is, altered to become magnesium dominated) resulting in a positive neutron-density separation.

The presence of anhydrite was interpreted when the density log approached 2.98 g/cm^3 with exceedingly low gamma ray readings (<10 API). When available, an acoustic response of 50 μs/ft also helped to diagnose the presence of anhydrite. Halite was interpreted through a significant neutron-density separation as well as an acoustic response of 67 μs/ft. Other low-density salts and potash salts (radiogenic potassium salts) were interpreted through unique variations on these same characteristics, with further diagnostic indications provided through gamma ray readings (the details of which can be found in table 2).

2D seismic lines were used to test models which were produced based on petrophysical interpretation. The seismic dataset was acquired by WesternGeco on behalf of the North Sea Transition Authority in 2015 as part of their Frontiers Program. Top and base Zechstein well tops were acquired from the NSTA Data Centre (Brackenridge et al., 2018). Seismic data was normal polarity, zero phase and was interpreted in SLB's Petrel software. Depth conversion was undertaken and calibrated to the top and base Zechstein well tops. Seismically derived surfaces were imported from the same NSTA Data Centre to create a thickness map of the Zechstein across the greater MNSH region (fig. 3a). This map confirmed Jenyon's observations of shallow salt slopes on the eastern margin of the MNSH Seaway and allowed for a preliminary spatial understanding of Zechstein thickness characteristics.

This work also analysed core data acquired from a well situated at a strategic location in the Quadrant 29 Basin. A sample taken from the British Geological Survey's Core Store (Keyworth) at 2550m in well 29/27- 1 was processed into thin sections which were then studied. The sample's location and depth is marked in fig. 4a.

Well ID	Year	CALI (Caliper)	GR (Gamma Ray)	NPHI (Neutron Porosity)	RHOB (Density)	DT (Acoustic)
21/26- 1D	1968	✓	✓	x	✓	✓
26/08- 1	1992	✓	✓	✓	✓	✓
26/12- 1	1985	✓	✓	✓	✓	✓
26/14- 1	1984	✓	✓	✓	✓	✓
27/03- 1	1967	✓	✓	✓	✓	✓
27/10- 1	1970	✓	✓	x	✓	✓
28/12- 1	1971	✓	✓	x	x	✓
29/23- 1	1967	✓	✓	—	—	✓
29/27- 1	1987	—	✓	—	—	✓
36/13- 1	1967	✓	✓	x	✓	✓
36/15- 1	1967	✓	✓	✓	✓	✓
37/10- 1	1969	✓	✓	✓	✓	x
37/23- 1	1970	x	✓	x	x	✓
38/18- 1	1967	✓	✓	✓	✓	x
38/24- 1	1983	✓	✓	✓	✓	✓
41/08- 2	1995	✓	✓	✓	✓	✓
41/10- 1	1995	✓	✓	✓	✓	✓
42/09- 1	1997	✓	✓	✓	✓	✓
42/10a- 1	1982	✓	✓	✓	✓	✓
43/05- 1	1994	✓	✓	✓	✓	✓
43/06- 1	1997	✓	✓	✓	✓	✓
44/06- 1	1992	✓	✓	✓	✓	✓
44/07- 1	1968	✓	✓	x	x	✓

Table 1. *The data availability of the wells used in this study. Ticks indicate that the wireline log was acquired for the entire Zechstein interval. Dashes*

indicate partial coverage. Crosses indicate full absence of the log within the Zechstein interval.

Lithology	Chemical Formula	Gamma Ray (API)	Neutron porosity (cm^3/cm^3)	Density (g/cm^3)	Acoustic (µs/ft)
Limestone Φ=10%	$CaCO_3$	0	10	2.71	62
Dolomite Φ=10%	$CaMg(CO_3)_2$	0	13.5	2.85	58
Shales		80 - 150	2.2 - 2.75	25 - 60	70 - 150
Anhydrite	$CaSO_4$	0	-2	2.98	50
Gypsum	$CaSO_4 \cdot 2H_2O$	0	49	2.35	52.5
Halite	NaCl	0	-3	2.03	67
Tachyhydrite	$CaCl_2 \cdot 2MgCl_2 \cdot 12H_2O$	0	50+	1.67	77
Carnallite	$MgCl_2 \cdot KCl \cdot 6H_2O$	200	65	1.57	122
Sylvite	KCl	500	-3	1.86	78
Polyhalite	$2CaSO_4 \cdot MgSO_4 \cdot K_2SO_4 \cdot H_2O$	190	15	2.79	57.5

Table 2. *The properties of key lithologies interpreted in this study after Taylor (1993), Rider (2002), Warren (2016) and SaltWorkConsultants (2023).*

4. RESULTS AND INTERPRETATION

This study presents five well correlation panels from across the greater MNSH region. Well correlation panels A and B (fig. 4a and 4b) display data from the

Northern Zechstein Basin (Quadrants 21, 26-29) and Southern Zechstein Basin (Quadrants 41-44), respectively (summarised in fig. 5a). These panels target basin environments and therefore avoid carbonate platforms and buildups. Every Zechstein halite formation (Z2 Stassfurt Halite Fm., Z3 Leine Halite Fm., and Z4 Aller Halite Fm.) is identified in both structural lows. The Stassfurt Halite Fm. is at its thickest in the Southern Zechstein Basin but is limited in the Northern Zechstein Basin. Instead, the Northern Zechstein Basin features extensive Z3 Leine Halite Fm. Well correlation panel C (fig. 4c) presents the two basinal wells from the Quadrant 38 Embayment (identified on the map in fig. 3b). The northern and southern ends of the embayment feature the same salt thickness trends as the Northern and Southern Zechstein Basins.

Well correlation panel D (fig. 4d) confirms the presence of the first four (Z1-Z4) Zechstein Cycles on the structurally elevated MNSH. Moreover, carbonates at the base of the cycles are almost always present albeit often limited in thickness. Well correlation panel E (fig. 4e) features localities from across the greater MNSH region where Z1 and Z2 carbonate platforms are capped with Z3 and Z4 halite. One key example is well 41/08- 2, where the carbonate to anhydrite ratio increases with each Zechstein cycle before then featuring 68m of the Z3 Leine Halite Fm. and 35m of the Aller Halite Fm (fig. 5b).

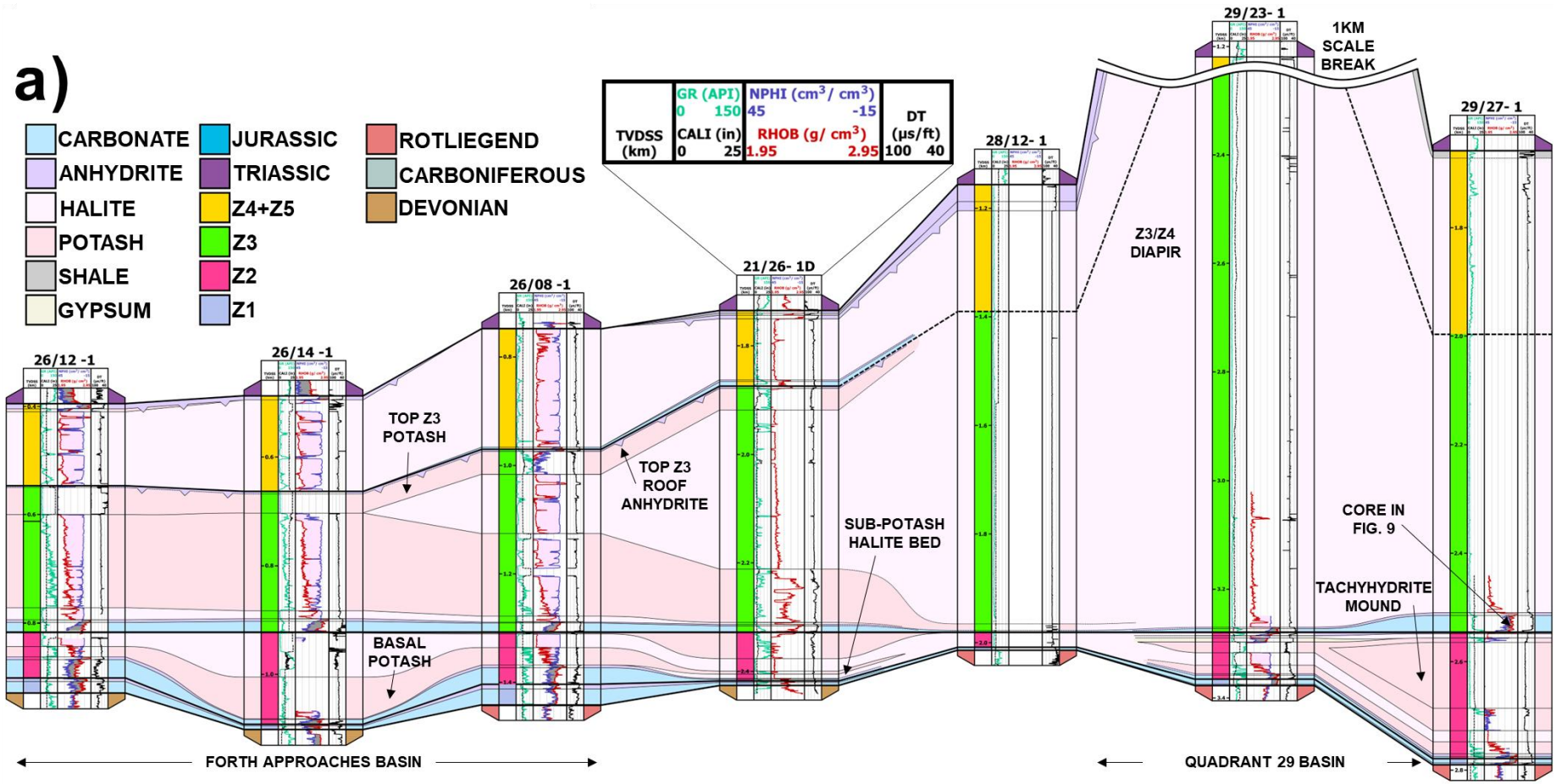
a)
CARBONATE
ANHYDRITE
HALITE
POTASH
SHALE
GYPSUM
JURASSIC
TRIASSIC
Z4+Z5
Z3
Z2
Z1
ROTLIEGEND
CARBONIFEROUS
DEVONIAN
TVDSS (km)
GR (API) 0 150
CALI (in) 0 25
NPHI (cm3/ cm3) 45 -15
RHOB (g/ cm3) 1.95 2.95
DT (µs/ft) 100 40
26/12 -1
26/14 -1
26/08 -1
21/26- 1D
28/12- 1
29/23- 1
29/27- 1
1KM SCALE BREAK
Z3/Z4 DIAPIR
TOP Z3 POTASH
TOP Z3 ROOF ANHYDRITE
SUB-POTASH HALITE BED
BASAL POTASH
CORE IN FIG. 9
TACHYHYDRITE MOUND
FORTH APPROACHES BASIN
QUADRANT 29 BASIN

b)

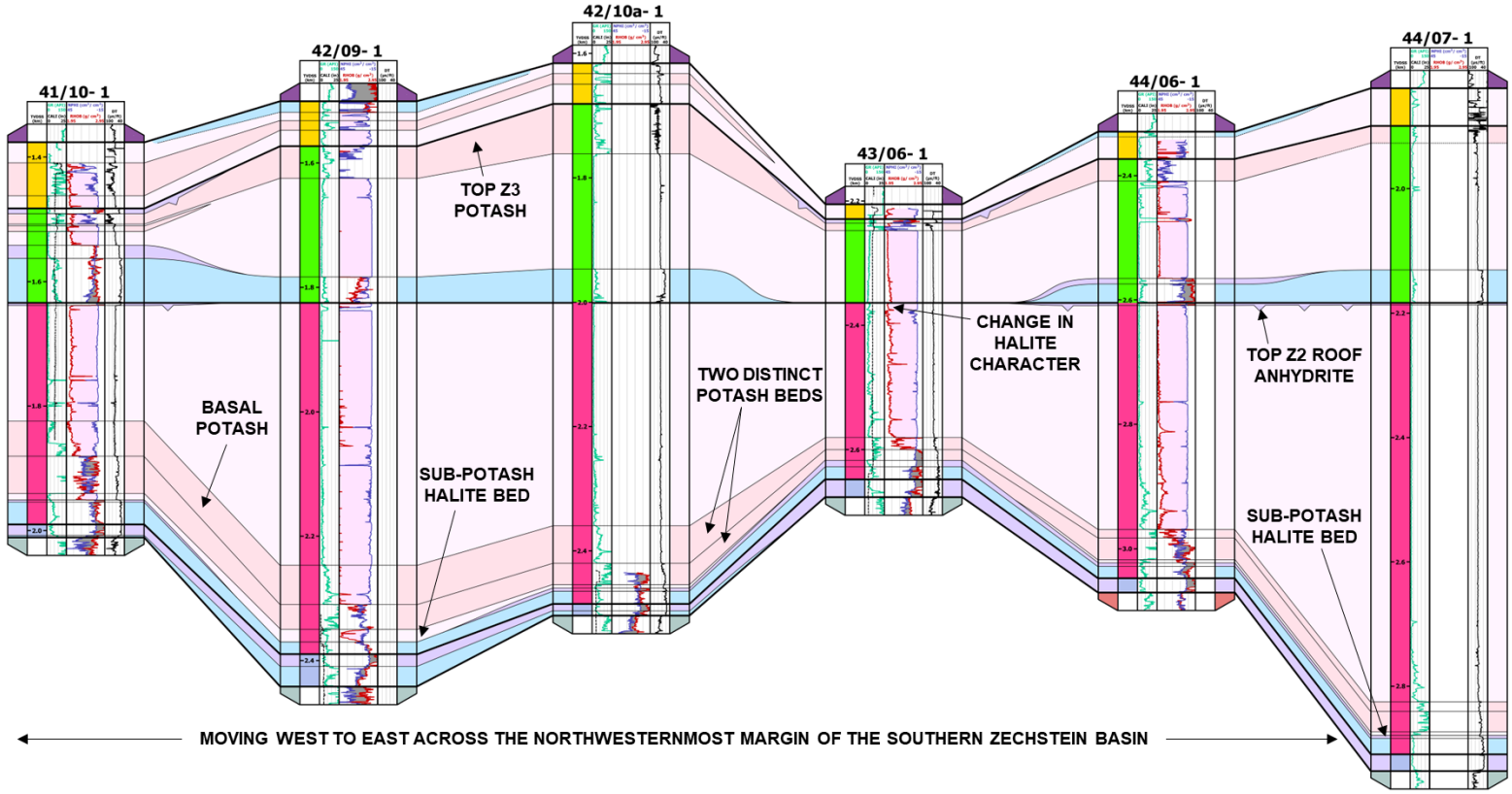
41/10- 1
42/09- 1
42/10a- 1
43/06- 1
44/06- 1
44/07- 1
TOP Z3 POTASH
BASAL POTASH
SUB-POTASH HALITE BED
TWO DISTINCT POTASH BEDS
CHANGE IN HALITE CHARACTER
TOP Z2 ROOF ANHYDRITE
SUB-POTASH HALITE BED
MOVING WEST TO EAST ACROSS THE NORTHWESTERNMOST MARGIN OF THE SOUTHERN ZECHSTEIN BASIN

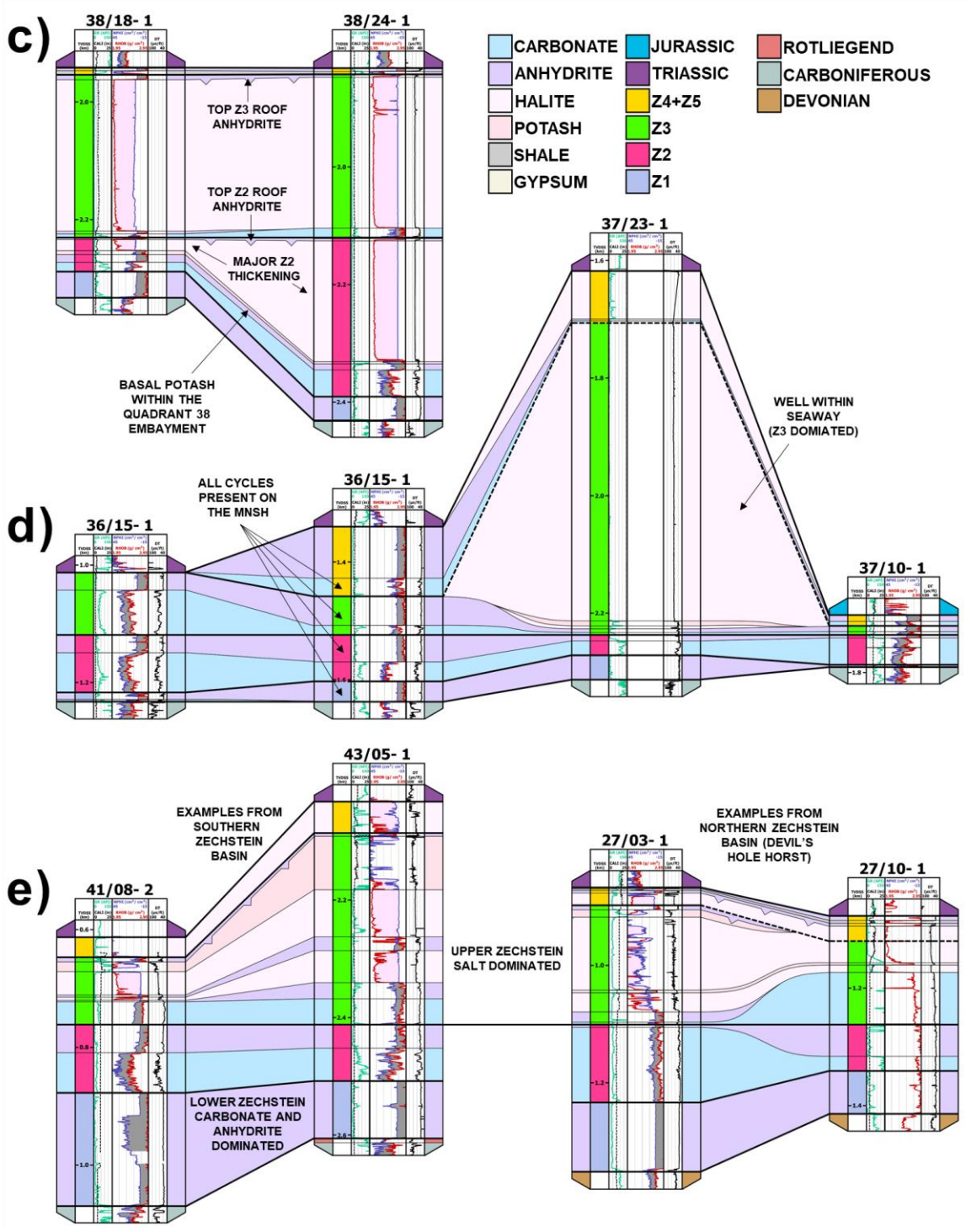

Fig. 4. *Well correlation panels across the greater MNSH region* ***a)*** *The Northern Zechstein Basin* ***b)*** *The Southern Zechstein Basin* ***c)*** *The Quadrant 38 Embayment* ***d)*** *The MNSH structural high and within the MNSH Seaway* ***e)*** *The salt-drowned platfroms from across the greater MNSH region.The left*

panel shows examples from the south, whilst the right panel shows examples from the north.

a)

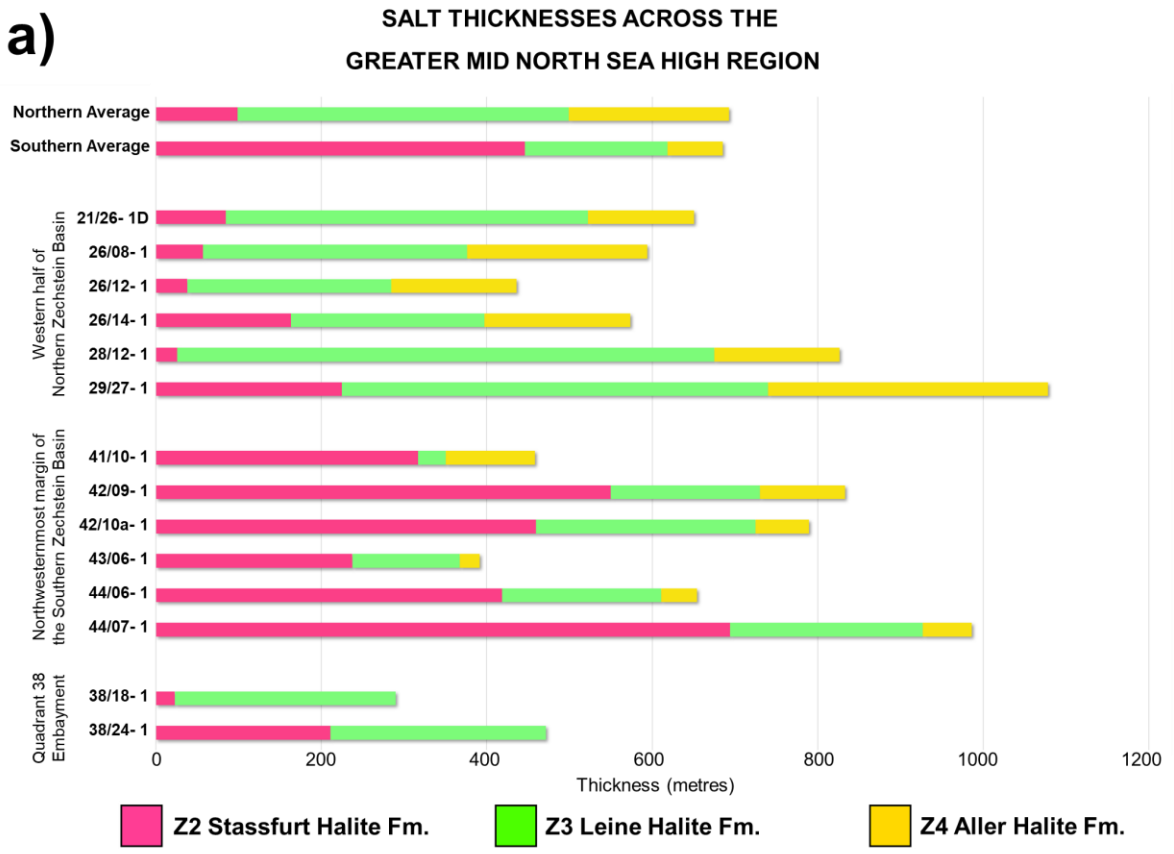
SALT THICKNESSES ACROSS THE
GREATER MID NORTH SEA HIGH REGION
Northern Average
Southern Average
Western half of Northern Zechstein Basin
21/26- 1D
26/08- 1
26/12- 1
26/14- 1
28/12- 1
29/27- 1
Northwesternmost margin of the Southern Zechstein Basin
41/10- 1
42/09- 1
42/10a- 1
43/06- 1
44/06- 1
44/07- 1
Quadrant 38 Embayment
38/18- 1
38/24- 1
0
200
400
600
800
1000
1200
Thickness (metres)
Z2 Stassfurt Halite Fm.
Z3 Leine Halite Fm.
Z4 Aller Halite Fm.

b)

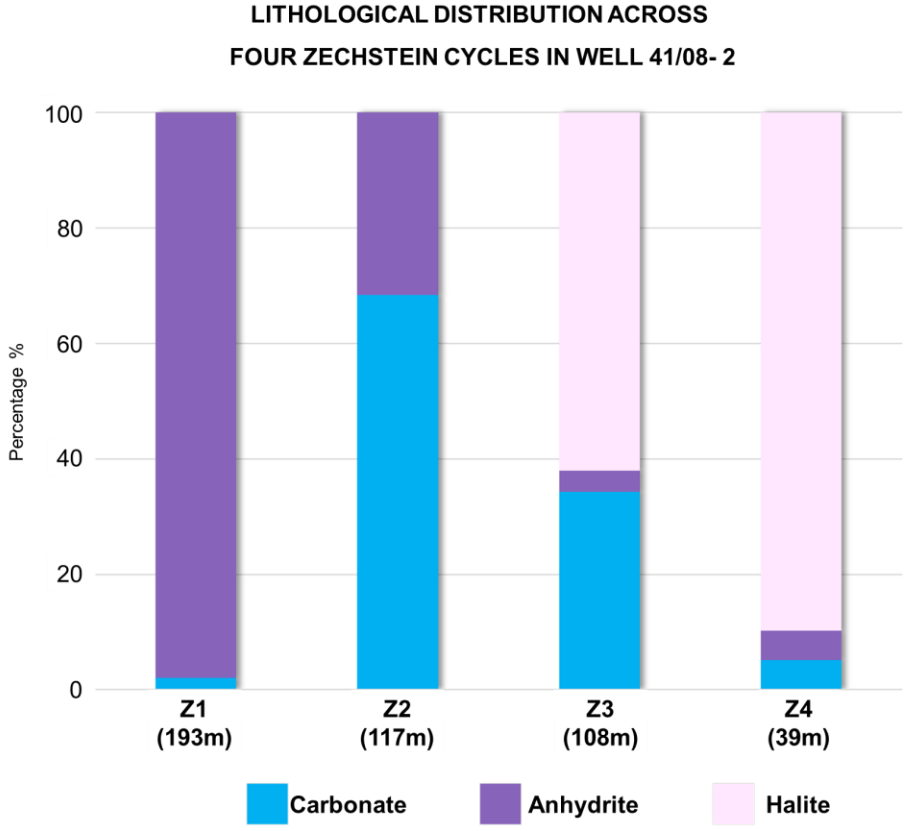
LITHOLOGICAL DISTRIBUTION ACROSS
FOUR ZECHSTEIN CYCLES IN WELL 41/08- 2
Percentage %
100
80
60
40
20
0
Z1
(193m)
Z2
(117m)
Z3
(108m)
Z4
(39m)
Carbonate
Anhydrite
Halite

Fig. 5. *Graphs summarising the petrophysical analysis* ***a)*** *Salt thickness across the Z2, Z3 and Z4 cycles for Fig. 4a, 4b, and 4c. The total average salt thickness is comparable across the study area with the only difference being which Zechstein cycle provides the salt. Well 29/23- 1 was removed from this average because it intersects a major salt diapir and therefore skews the data* ***b)*** *Facies transition across Zechstein cycles in well 41/08- 2.*

Three seismic lines were interpreted to verify the accuracy of the petrophysical interpretation and to confirm whether the spatial variation in the described facies distribution occurred within the MNSH Seaway. The Z1 and Z2 (Wuchiapingian) stratigraphy and the Z3 and Z4 (Changhsingian) stratigraphy are partitioned by the distinct reflector at the top Z2 Stassfurt Halite Fm./base Z3 Plattendolomit Fm. Seismic line X (fig. 6a) displays the Quadrant 29 Basin just to the MNSH Seaway. Here, the Z2 Stassfurt Halite Fm. package is consistently thin. The package thickness varies in association with tachyhydrite salt mounds, with a continuous overlying Z3 Plattendolomit Fm. package; nonetheless, this thickening is of little significance when compared to the huge overlying Z3 and Z4 halite package. Seismic line Y (fig. 6b) transects the middle of the MNSH Seaway and the flanking MNSH platforms. Here the Z2 Stassfurt Halite Fm. package is extremely thin, and the seaway infill is comprised solely of Z3 and Z4 halite. The Z2 Stassfurt Halite Fm. package varies along seismic line Z (fig. 6c): The package is thick in the Southern Zechstein Basin but disappears on the Orchard Platform, with minor shows of the Z2 halite re-entering in the southern part of the Seaway. Ultimately, the seismic data demonstrates that the same regional trends in salt thicknesses are apparent within the MNSH Seaway.

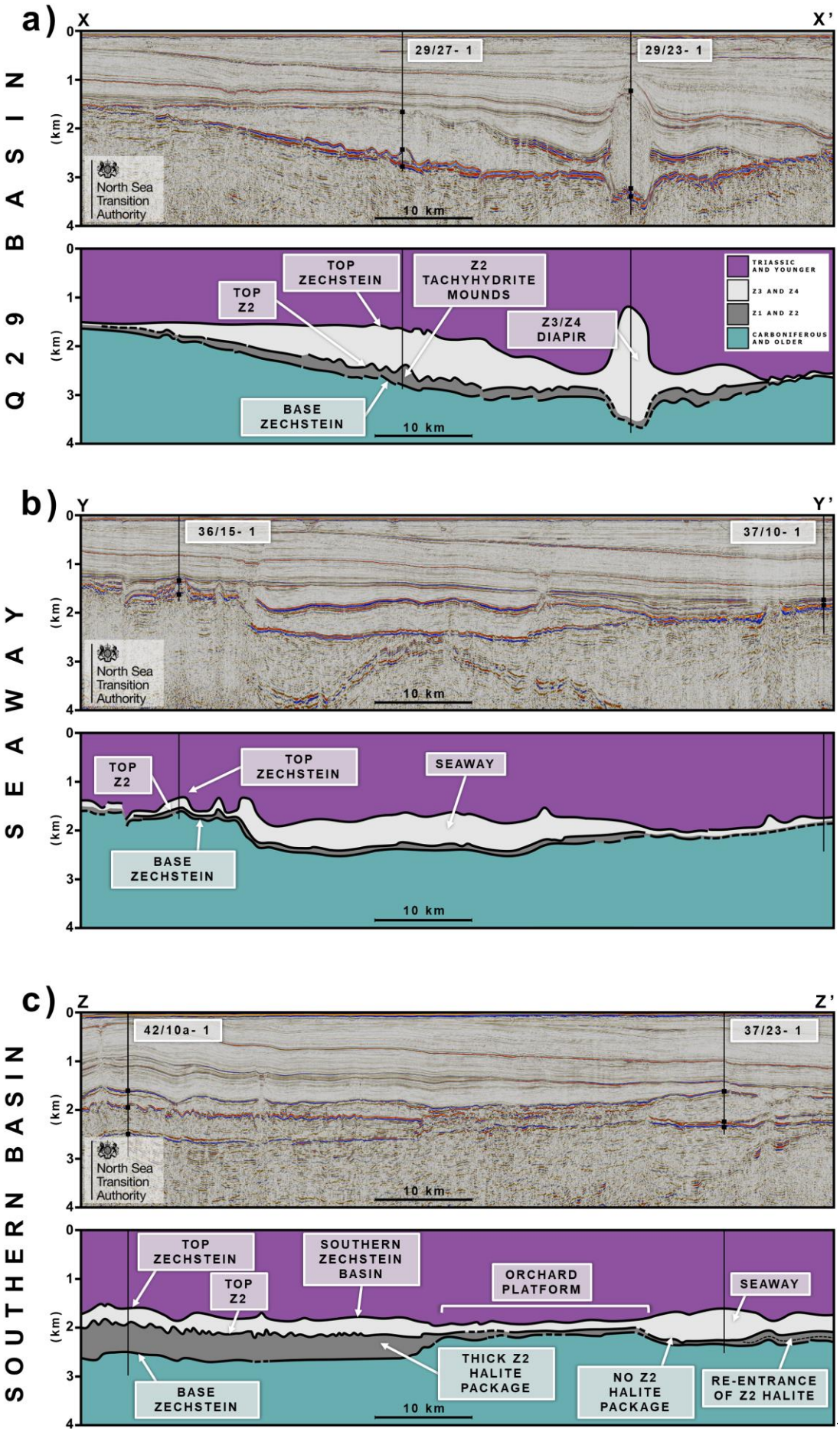
a)
X
X'
29/27- 1
29/23- 1
North Sea Transition Authority
10 km
(km)
Q29 BASIN
TOP ZECHSTEIN
Z2 TACHYHYDRITE MOUNDS
TOP Z2
Z3/Z4 DIAPIR
BASE ZECHSTEIN
TRIASSIC AND YOUNGER
Z3 AND Z4
Z1 AND Z2
CARBONIFEROUS AND OLDER
b)
Y
Y'
36/15- 1
37/10- 1
SEAWAY
c)
Z
Z'
42/10a- 1
37/23- 1
SOUTHERN BASIN
SOUTHERN ZECHSTEIN BASIN
ORCHARD PLATFORM
THICK Z2 HALITE PACKAGE
NO Z2 HALITE PACKAGE
RE-ENTRANCE OF Z2 HALITE

Fig. 6. *Seismic evidence for the salt distributions observed in petrophysical data. Seismic depth conversion is accurate for Zechstein well tops. In general, the Z2 Stassfurt Halite Fm. thins in the MNSH Seaway and Northern Zechstein Basin, which suggests that petrophysical correlation alone is sufficient to provide insight into marine gateways. Locations of seismic lines are available in fig. 3b* ***a)*** *Seismic line X across the Quadrant 29 Basin (where the MNSH Seaway meets the Northern Zechstein Basin)* ***b)*** *Seismic line Y through the MNSH Seaway* ***c)*** *Seismic line Z from the Southern Zechstein Basin to the MNSH Seaway via the Orchard Platform.*

4.1. Z2 Stassfurt Halite Fm. variability.

The base of the Z2 Stassfurt Halite Fm. is marked by a distinct drop in density from the underlying Zechstein stratigraphy. It is the first major halite package across the greater MNSH region, save for local Werrahalit Fm. pods (Underhill and Hunter, 2008). The top of the Z2 Stassfurt Halite Fm. is often marked through roof anhydrite (Deckanhydrit Mbr.); otherwise, the Z3 Plattendolomit Fm. marks the top of the Z2 Stassfurt Halite Fm. The only exception is found in well 43/06- 1, where there is no clear lithological buffer between the Z2 Stassfurt Halite Fm. and the Z3 Leine Halite Fm; nevertheless, the data shows a change in halite characteristics (indicated in fig. 4b). The Z2 Stassfurt Halite Fm. features packages with higher gamma ray and density readings which together indicate the presence of potash beds (table 2). This contrasts with the consistent wireline responses in the overlying Leine Halite Fm., which suggests a greater halite purity.

The Z2 Stassfurt Halite Fm. exhibits extensive regional thickness variability. Across the Northern Zechstein Basin, the average thickness of this unit is

99m; however, the Southern Zechstein Basin demonstrates a far greater average thickness of 456m. Within the MNSH Seaway, well 37/23- 1 yields no clear evidence for the Z2 Stassfurt Halite Fm.; despite this, seismic data suggest that this formation does occur in the eastern parts of the seaway. Regionally, the base of the Z2 Stassfurt Halite Fm. features beds of potash salts that are up to 50m thick. The potash salts are often underlain by an unsubstantial (<30m) bed of halite; moreover, the entire package thins in the east toward Dogger Bank in Quadrant 44. There is no evidence for a potash salt package at the roof of the Z2 Stassfurt Halite Fm. Within the Quadrant 29 Basin, the Z2 Stassfurt Halite Fm. features the rare evaporitic mineral tachyhydrite (indicated in fig. 4a and 6a) which was first interpreted and discussed by Taylor (1993).

4.2. Z3 Leine Halite Fm. variability.

The Z3 Plattendolomit Fm. and Z3 Hauptanhydrit Fm. provide a regionally identifiable petrophysical contrast to interpret the base of the Z3 Leine Halite Fm. Across the greater MNSH region the top of the Z3 Leine Halite Fm. is often emphasised by an unnamed Z3 Roof Anhydrite Mbr. (that is, the Z3 equivalent to the Z2 Deckanhydrit Mbr). The Quadrant 29 Basin remains the only part of the greater MNSH region where confidence wanes for the top Z3 pick. An average thickness of 400m was found for the Z3 Leine Halite Fm. in the Northern Zechstein Basin, whilst this average was 172m in the Southern Zechstein Basin. Within the MNSH Seaway, the Z3 Leine Halite Fm. thickness was 520m whilst the Quadrant 38 Embayment demonstrated an average of 264m (+/- 3m).

4.3. Z4 Aller Halite Fm. variability.

In the Quadrant 29 Basin, the base of the Z4 Aller Halite Fm. is often difficult to identify due to limited data availability and absent petrophysical contrast to the underlying Z3 Leine Halite Fm. The Z4 Aller Halite Fm. yields an average thickness of 67m in the Southern Zechstein Basin but is absent across the entire Quadrant 38 Embayment. In the Northern Zechstein Basin, this formation has an average thickness of 194m. This is the least substantial major halite package across the greater MNSH region.

5. DISCUSSION

5.1. Halite formation thickness disparity.

The results show that the primary disparity between the Northern and Southern Zechstein Basins centres around the Z2 Stassfurt Halite Fm. Regional controls not only influence thickness variations but also minerology and facies characteristics.

Current understanding suggests that the Northern Panthalassic Ocean connected to the Northern Zechstein Basin via the Boreal Seaway, and that a Southern Zechstein Basin connection to the Eastern Palaeo-Tethys Ocean was limited or absent (Ziegler, 1988; Sørensen et al., 2007; shown in fig. 1). It is therefore likely that when the Northern Zechstein Basin featured elevated salinity, the Southern Zechstein Basin would have displayed the same. During these periods of elevated salinity in the north, normal salinity in the Southern Zechstein Basin would only be possible if there was a major connection to the Eastern Palaeo-Tethys Ocean.

Tucker (1991) describes two contrasting sequence stratigraphic successions in restricted basins: one scenario involves incomplete drawdown and the other

features complete drawdown with wholesale basin desiccation from evaporation. With this in mind, the distribution of the Z2 Stassfurt Halite Fm. suggests different evaporation characteristics in each basin. The limited thickness of the Z2 Stassfurt Halite Fm. in the Northern Zechstein Basin suggests a less evaporitic environment whilst the opposite is true for the Southern Zechstein Basin (fig. 7). If the two basins were in full communication, then the data would show similar thickness distributions. The discrepancy in the Z2 Stassfurt Halite Fm. thickness was first noted by Taylor (1993). Our current study has investigated trends in salt thickness at a larger scale and provided a palaeoenvironmental explanation for regional variation.

The Z2 Hauptdolomit Fm. carbonates remain present across the structurally elevated MNSH (fig. 4d), which indicates that at Z2 highstand the MNSH was covered by a shallow water column to allow for carbonate progradation (in line with the petrophysical interpretation of Patruno et al., 2017). Nonetheless, as Z2 evaporation commenced, a lack of halite on the MNSH suggests that communication between the Northern and Southern Zechstein Basins was restricted to the MNSH Seaway: The ever-decreasing width of the MNSH Seaway limited fluid exchange between the basins. As such, hypersalinity, caused by reduced volumes of marine water reaching the Southern Zechstein Basin, catalysed the precipitation of the extensive salt deposit found there (Sarg, 2001; fig. 8). Comparable Z3 and Z4 halite thicknesses across both basins suggests restored communication following Z2 isolation.

Van de Belt and de Boer (2007) present a “shallow-basin model” for the Southern Zechstein Basin. Essentially, salt precipitation continuously added weight to the overburden which drove basin subsidence (becoming a self-sustaining feedback loop). Moreover, they (ibid.) suggest that a shallow basin is in fact preferable for the precipitation of thick salt sequences and their

model reduces the need for replenishment via repeated opening and closing of major marine connections. Their model (ibid.) supports the work presented in this study as we suggest that the MNSH Seaway provided a continuous (albeit limited) trickle of marine water into the Southern Zechstein Basin. With the “shallow-basin model” in mind, the regional variation in Z2 halite precipitation could suggest that the Southern Zechstein Basin underwent most subsidence in the late Z2 cycle due to the weight of salt. However, the Northern Zechstein Basin probably experienced a later phase of subsidence as most salt was produced in Z3 and Z4 times. This confirms the preliminary suggestion by Taylor (1993) that the limited Z2 Stassfurt Halite Fm. in the Northern Zechstein Basin was controlled by primary depositional factors opposed to secondary salt migration.

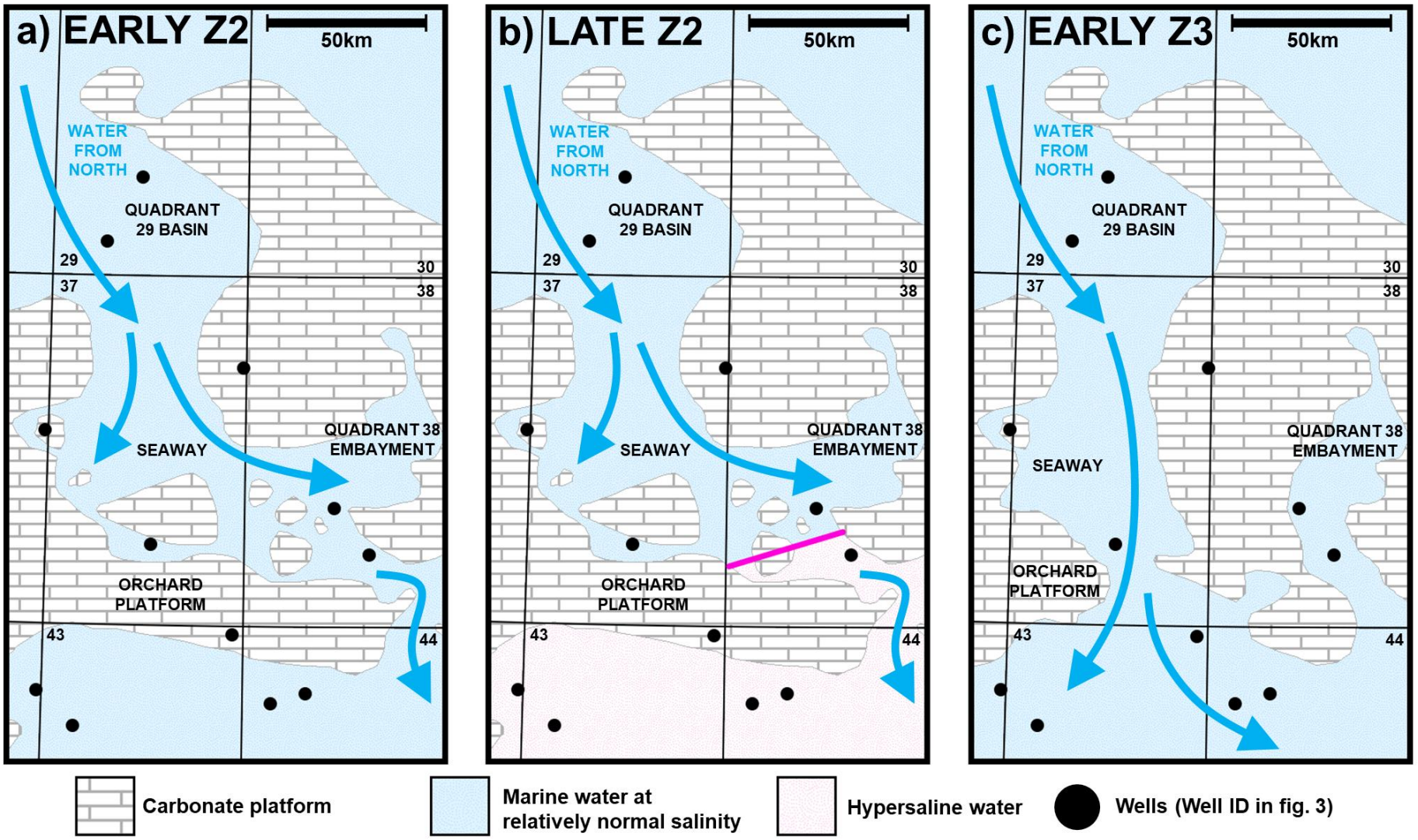
a) EARLY Z2
50km
WATER FROM NORTH
QUADRANT 29 BASIN
29
30
37
38
SEAWAY
QUADRANT 38 EMBAYMENT
ORCHARD PLATFORM
43
44
b) LATE Z2
50km
WATER FROM NORTH
QUADRANT 29 BASIN
29
30
37
38
SEAWAY
QUADRANT 38 EMBAYMENT
ORCHARD PLATFORM
43
44
c) EARLY Z3
50km
WATER FROM NORTH
QUADRANT 29 BASIN
29
30
37
38
SEAWAY
QUADRANT 38 EMBAYMENT
ORCHARD PLATFORM
43
44
Carbonate platform
Marine water at relatively normal salinity
Hypersaline water
Wells (Well ID in fig. 3)

Fig. 7. *Palaeogeographical evolution of the MNSH Seaway based on petrophysical interpretations. The pink line indicates the approximate separation between the basins based on petrophysical data. Maps of carbonate platforms after Brackenridge et al. (2020), Garland et al. (2023), and Browning-Stamp et al. (2023).*

5.2. Regional Z2 basal potash to refine basin communication model.

Potash salts (KCl) should precipitate after halite (NaCl) in models for brine evolution (Habicht, 1979). This is the case for the Z3 Leine Halite Fm., where the Southern Zechstein Basin and much of the Northern Zechstein Basin feature potash salt above halite (as indicated in fig. 4a and 4b. and summarised in fig. 8).

The basal Z2 Stassfurt Halite Fm. potash salts provide further geochemical evidence to constrain the timings of restriction and communication. All wells studied in the Southern Zechstein Basin feature the basal Z2 potash (in line with detailed analysis by Garland et al., 2023). Furthermore, the basal potash facies is present in the Quadrant 29 Basin and the Forth Approaches Basin (key palaeo-lows within the Northern Zechstein Basin), but current petrophysical data does not reveal the presence of the basal potash within the MNSH Seaway (fig. 4d). Across the study area, a thin layer of halite often occurs beneath the potash salts. This suggests that a regionally continuous albeit limited phase of halite precipitation occurred before the potash phase, indicating a period of elevated aridity because the entire brine evolution model has been rapidly fulfilled. Warren et al. (2016) suggests that the Southern Zechstein Basin Z2 basal potash is a replacement of the original halite; however, this assessment explains neither the halite bed which underlies the

Z2 potash, nor the primary potash precipitation geometry discussed by Garland et al. (2023). Following this, both basins entered a second halite phase where the Southern Zechstein Basin developed thick accumulations of the Z2 Stassfurt Halite Fm.

It is presumed that the lowest relative sea-level occurred during regional potash precipitation (fig. 8b). After its deposition, there was a slight rise in relative sea-level to allow for the minor freshening event in the Southern Zechstein Basin (fig. 8c), something which only added to the remaining brine in the basin. The net geochemistry of fresh seawater mixed with concentrated brine resulted in basin conditions that were still too severe to begin a new carbonate cycle but were conducive for a new phase of halite precipitation (fig. 8c). The effects of depleted potassium concentrations in the early Z2 Stassfurt Halite Fm. times due to previous potash precipitation were still felt at the end of Z2 evaporation: The net depletion of potassium in the basin prevented a second phase of potash precipitation which resulted in a pure halite phase for the remainder of Z2 times. As such, the Z2 Stassfurt Halite Fm. can be separated into two cycles corresponding to restriction from different seaways: The first cycle featured the precipitation of a vast potash system (corresponding to restriction in the Boreal Seaway) during a period of elevated aridity, whilst the second cycle allowed for typical halite precipitation (amplified in the Southern Zechstein Basin by restriction due to the MNSH Seaway). As discussed, a contrasting precipitation system is present within the Z3 Leine Halite Fm. as the geochemistry of the water allowed for the standard potash phase at the top of the Z3 evaporite column (indicated in fig. 4a and 4b). The only exception in Z3 times is found in the Forth Approaches Basin (Brackenridge et al., 2023) where local conditions seem to have

amplified potassium concentrations resulting in great accumulations of potash salts throughout Zechstein deposition (fig. 4a).

5.3. Salt-drowned platforms

In Z1 and Z2 (Wuchiapingian) times, carbonate platforms developed in Quadrants 41, 42 and 43 on the northwesternmost margin of the Southern Zechstein Basin (Patruno et al., 2017). Recent exploration at the Ossian and Pensacola discoveries has revealed promising reservoir play opportunities within this area (Browning-Stamp et al., 2023; Garland et al., 2023). Petrophysical data shows that some platforms were unaffected by Z2 evaporation in the Southern Zechstein Basin during which time significant halite precipitation occurred around the platforms but not on top of them (fig. 4e). This indicates a potential phenomenon that may have promoted subaerial exposure during Z2 evaporation before the platforms were then drowned in halite during Z3 and Z4 times (Changhsingian). Critically, this trend is also apparent in the Northern Zechstein Basin (as indicated in fig. 4e).

Our regional petrophysical analysis and resultant mapping offers evidence in line with the argument for Z3 sea-level rise (as described by van Wees et al., 2000, and McKie, 2017). Rather than halite precipitation in one basin, a regional blanket of Z3 and Z4 halite exists which directly contrasts the lateral characteristics of the Z2 halite (fig. 8). The MNSH Seaway controlled the replenishment of seawater to the Southern Zechstein Basin during Z2 times, but this system had no influence in the late Zechstein. Sea-level rise drowned any isolated platforms and buildups resulting in Z3 and Z4 halite precipitation even on Z1 and Z2 carbonates (fig. 4e, 6c and 7). The seaway was overwhelmed by sea-level rise which restored full communication between the

Northern and Southern Zechstein Basins, thus ending the Z2 basin isolation system.

Smith and Taylor (1989) use the MNSH Seaway as an analogue to infer the presence of another potential marine connection between the Northern and Southern Zechstein Basins which could reside between the eastern coastline of the UK and the MNSH. When examined in isolation, the presence of halite within well 41/08- 2 could suggest a narrow extension of the Southern Zechstein Basin into the MNSH structure within Quadrant 41. Nonetheless, as this study identifies an absence of Z2 halite within this well, the potential feature was not present in times of early Zechstein deposition. As such, the feature is unlikely to be akin to the MNSH Seaway which was established as a gap in the MNSH before Zechstein deposition. Ultimately, that the halite found in well 41/08- 2 correlates to the later Z3 and Z4 cycles when sea-level rise refilled the Southern Zechstein Basin (fig. 4e).

The Zechstein maps of Doornenbal and Stevenson (2010) show reasonably thick Zechstein accumulations (up to approximately 600m) through the Ringkøbing Fyn High with a strike parallel to that of the MNSH Seaway. With this in mind, whilst other seaways could have connected the Northern and Southern Zechstein Basins, it has yet to be established whether these are primary features or salt filled Mesozoic grabens.

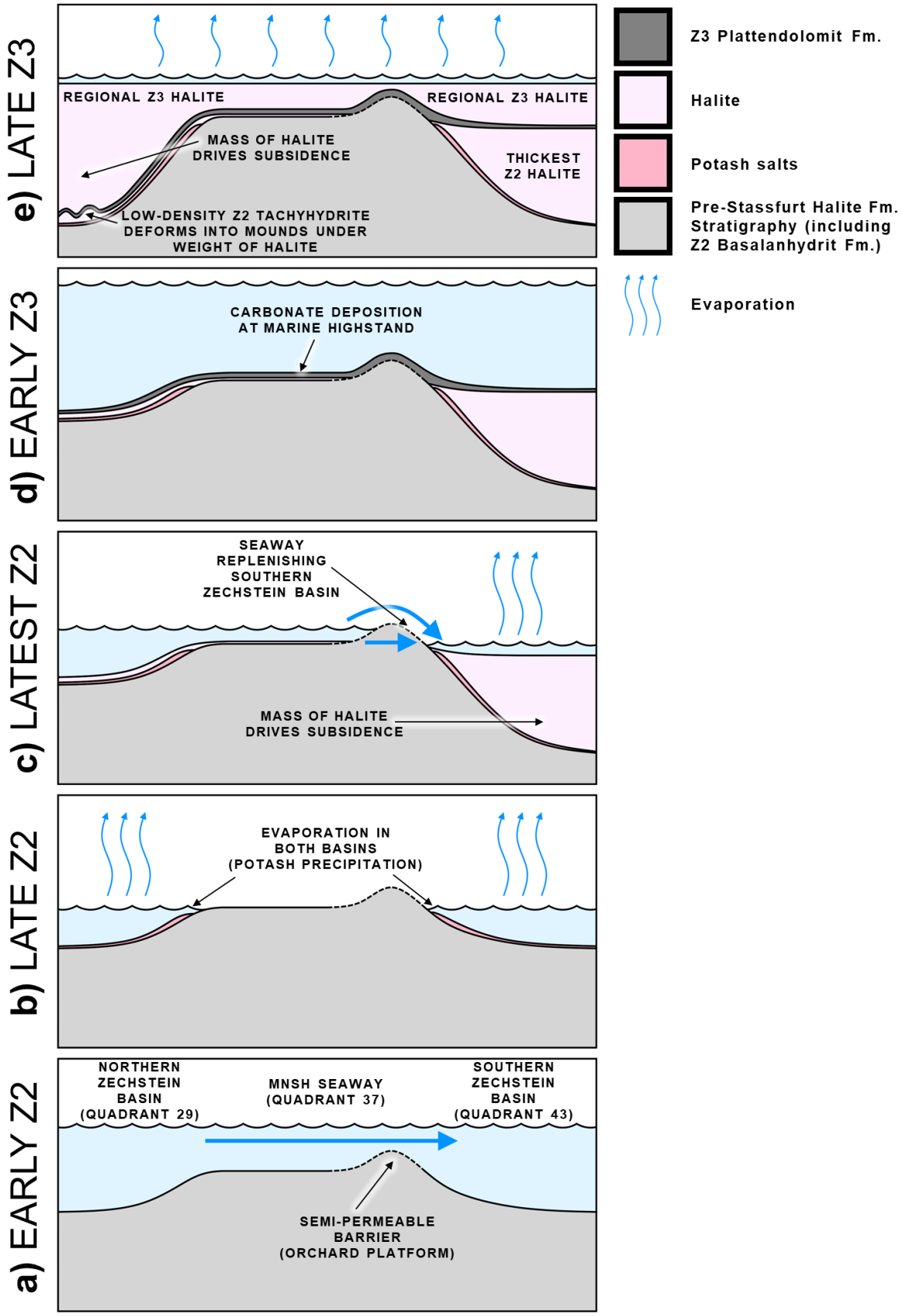
e) LATE Z3
REGIONAL Z3 HALITE
REGIONAL Z3 HALITE
MASS OF HALITE DRIVES SUBSIDENCE
THICKEST Z2 HALITE
LOW-DENSITY Z2 TACHYHYDRITE DEFORMS INTO MOUNDS UNDER WEIGHT OF HALITE
d) EARLY Z3
CARBONATE DEPOSITION AT MARINE HIGHSTAND
c) LATEST Z2
SEAWAY REPLENISHING SOUTHERN ZECHSTEIN BASIN
MASS OF HALITE DRIVES SUBSIDENCE
b) LATE Z2
EVAPORATION IN BOTH BASINS (POTASH PRECIPITATION)
a) EARLY Z2
NORTHERN ZECHSTEIN BASIN (QUADRANT 29)
MNSH SEAWAY (QUADRANT 37)
SOUTHERN ZECHSTEIN BASIN (QUADRANT 43)
SEMI-PERMEABLE BARRIER (ORCHARD PLATFORM)
Z3 Plattendolomit Fm.
Halite
Potash salts
Pre-Stassfurt Halite Fm. Stratigraphy (including Z2 Basalanhydrit Fm.)
Evaporation

Fig. 8. *Evolution of the MNSH Seaway across the Z2 and Z3 cycles. Subsidence of Southern Zechstein Basin is in line with the model by Van de Belt and de Boer (2007), which has then been applied to the Northern Zechstein Basin.*

5.4. Stratigraphic evolution of the Quadrant 38 Embayment.

Despite appearing regionally insignificant, the Quadrant 38 Embayment provides critical further evidence which supports the models of Southern Zechstein Basin Z2 hypersalinity and post-Z2 relative sea-level rise. Whilst the Quadrant 38 Embayment generally shows a north-south trend (fig. 3b and 7c), in Z2 times the Orchard Platform developed into the embayment (fig. 7a and b).

There are two basinal wells located in the Quadrant 38 Embayment to the north and south of the elevated structure (38/18- 1 and 38/24- 1, shown in fig. 4c). The petrophysical data from these wells confirms contrasting facies distribution across the embayment. Being only 19km apart, the proximity between these wells allows for confidence in the facies correlation.

The limits of the Z2 cycle are clear and consistent across both wells: The base of the Z2 Hauptdolomit Fm. follows the distinct characteristics of the Z1 Werraanhydrit Fm., and a substantial and laterally consistent roof anhydrite (Z2 Deckanhydrit Mbr.) marks the end of the Z2 cycle. The thickness of the Z2 Stassfurt Halite Fm. is the only discrepancy between these wells. In the north this formation is very thin (23m in 38/18- 1, fig. 5a) compared to the extensive halite accumulations found to the south (219m in 38/24- 1, fig. 5a). In both wells, the Z2 Stassfurt Halite Fm. sits on a gamma ray spike correlating to a thin bed of the basal potash salt. Combing the above confirms that the

formation precipitated over the same time scale. As demonstrated by thick (and equal) successions of Z3 Leine Halite Fm. (indicated in fig. 4c and 5), well 38/18- 1 did not suffer from a lack of accommodation space. Accordingly, the north of the Quadrant 38 embayment did not maintain the same salinity as the rest of the Southern Zechstein Basin in Z2 times.

The mapped entrance to the embayment resides in the southeast of the study area (fig. 3a and 3b) which initially suggests that the feature was part of the Southern Zechstein Basin. However, if the Orchard Platform (Z2 Hauptdolomit Fm.) restricted the southern part of the Quadrant 38 Embayment (as suggested by the 3D seismic interpretation of Browning-Stamp et al., 2023 and Garland et al., 2023), this would explain the variation in Z2 facies distribution over such a short distance. As such, it would appear that the north of the embayment was replenished by the MNSH Seaway throughout Z2 evaporation, leaving the south of the embayment to undergo the same hypersalinity as the Southern Zechstein Basin (fig. 7).

Following this complicated local palaeoenvironmental history in Z2 times (fig. 7), the entirety of the Quadrant 38 Embayment is uniformly blanketed with Z3 Leine Halite Fm. (indicated in fig. 4c). This supports the argument for early Z3 relative sea-level rise as another Zechstein isolation system is made redundant, giving way to regionally uniform halite precipitation.

5.5. Occurrence of tachyhydrite in the Northern Zechstein Basin

Mulholland et al. (2018) offer different conclusions for Permian basin communication in their study which mapped a Z1-Z2 platform across the southern region of the MNSH Seaway. New seismic data allowed the characteristics of this platform to be mapped in greater detail by Browning-

Stamp et al. (2023) and Garland et al. (2023) (fig. 7). Mulholland et al. (2018) suggest that the Northern Zechstein Basin became hypersaline (or “crystal starved”) in Z2 times, the opposite of which is suggested here. Not only does this idea stray from the current suggestions regarding late Permian marine connections, but it also conflicts with petrophysical evidence for Z2 halite thicknesses. Their primary evidence for the Northern Zechstein Basin becoming hypersaline is based on the evaporitic mineral tachyhydrite (the properties of which can be found in table 2). Tachyhydrite was first identified using petrophysical responses in well 29/27- 1 by Taylor (1993), where a structure with reef-like seismic geometry was targeted for hydrocarbon exploration. Instead of Z2 Hauptdolomit Fm. reef facies, the well discovered a mound of tachyhydrite (first described by Taylor, 1993); later, the entire mound system was mapped by Mulholland et al. (2018). In theory, tachyhydrite could perhaps precipitate in the late stages of brine evolution (Warren, 2016), and therefore models of wholesale basin desiccation were invoked; however, emerging research (e.g. Sørensen et al., 2007; McKie, 2017) suggests that this is unlikely. Nonetheless, this study has shown that it was in fact the Southern Zechstein Basin that was hypersaline in late Z2 times, and therefore the question of the occurrence of tachyhydrite must still be answered.

Warren (2017) provides a thorough analysis of tachyhydrite properties. Notably, tachyhydrite crystals enter a liquid phase when reacting with moisture in the air and it never forms a bed with primary precipitation textures. Cheng et al. (2019) provides a detailed evaluation of tachyhydrite precipitation conditions. Critically, they (ibid.) evidence that brine evolution can never form tachyhydrite due to the lack of sufficient volumes of calcium chloride in brine, not to mention the unique humidity, temperature and pressure conditions required for the precipitation of this mineral. Their study shows that

tachyhydrite cannot precipitate even as an end member of brine evolution and point to hydrothermal fluids to source the calcium chloride required for tachyhydrite alteration. The emerging understanding of tachyhydrite conditions allowed for a re-evaluation of its presence in the Northern Zechstein Basin.

The tachyhydrite is only found within the Quadrant 29 Basin which sits to the west of the Auk field where latest-Permian uplift and erosion caused karstification of the Zechstein carbonates found there (Trewin and Bramwell, 1991). Given that this structural high was tectonically active, enriched hydrothermal fluids could have migrated through the subsurface to replace halite seen in neighbouring wells. Such fluids could have originated from deep seated magma degassing in the subsurface (Lukanin, 2016), but further research is required to test this hypothesis.

Not only would this provide an alternative explanation for the presence of tachyhydrite, but it would also explain why it is locally restricted to the Quadrant 29 Basin: If Z2 hyper-salinity were to have occurred across the entire Northern Zechstein Basin, then the tachyhydrite should have precipitated within other palaeo-lows such as the Forth Approaches Basin. Taylor (1993) suggests that local igneous activity and basement faulting could have mobilised or precipitated the tachyhydrite. However, fluids derived from igneous intrusions were more likely to have altered halite to tachyhydrite.

Core samples from well 29/27- 1 were studied over the Z3 Plattendolomit Fm. interval above the tachyhydrite mound system. In contrast to the typical MNSH dolomite, the tests conducted using weak hydrochloric acid and alizarin-red solution revealed that this formation is overwhelmingly limestone-dominated within the Quadrant 29 Basin (fig. 9). Furthermore, this limestone is extremely dense and impermeable. Indeed, one fracture runs through the core with minor

dolomitisation on either side suggesting that the dolomitising fluids only penetrated a few millimetres into the limestone (fig. 9). As such, this limestone is essentially a caprock. Subsequently, hydrothermal fluids could have provided the calcium chloride required for secondary tachyhydrite alteration, yet the impermeable Z3 Plattendolomit Fm. shielded the overlying salts from becoming modified. Such a substantial volume (up to 274m in some cases, Taylor, 1993) of this unstable mineral simply could not have survived the subsequent Z3 flooding event without some kind of protective cap. The unusual mound-like structures developed due to the weaker tachyhydrite deforming under the weight of the overburden. More specifically, the tachyhydrite probably deformed during Z3 evaporation where the accumulating weight of the Z3 Leine Halite Fm. likely influenced basin subsidence (fig. 8, in line with the model of Van de Belt and de Boer, 2007). This hypothesis not only offers an explanation for the presence of the tachyhydrite, but also for the development of the mound-like structures alongside the consistent presence of the Z3 Plattendolomit Fm. above the mounds in seismic data (fig. 5a).

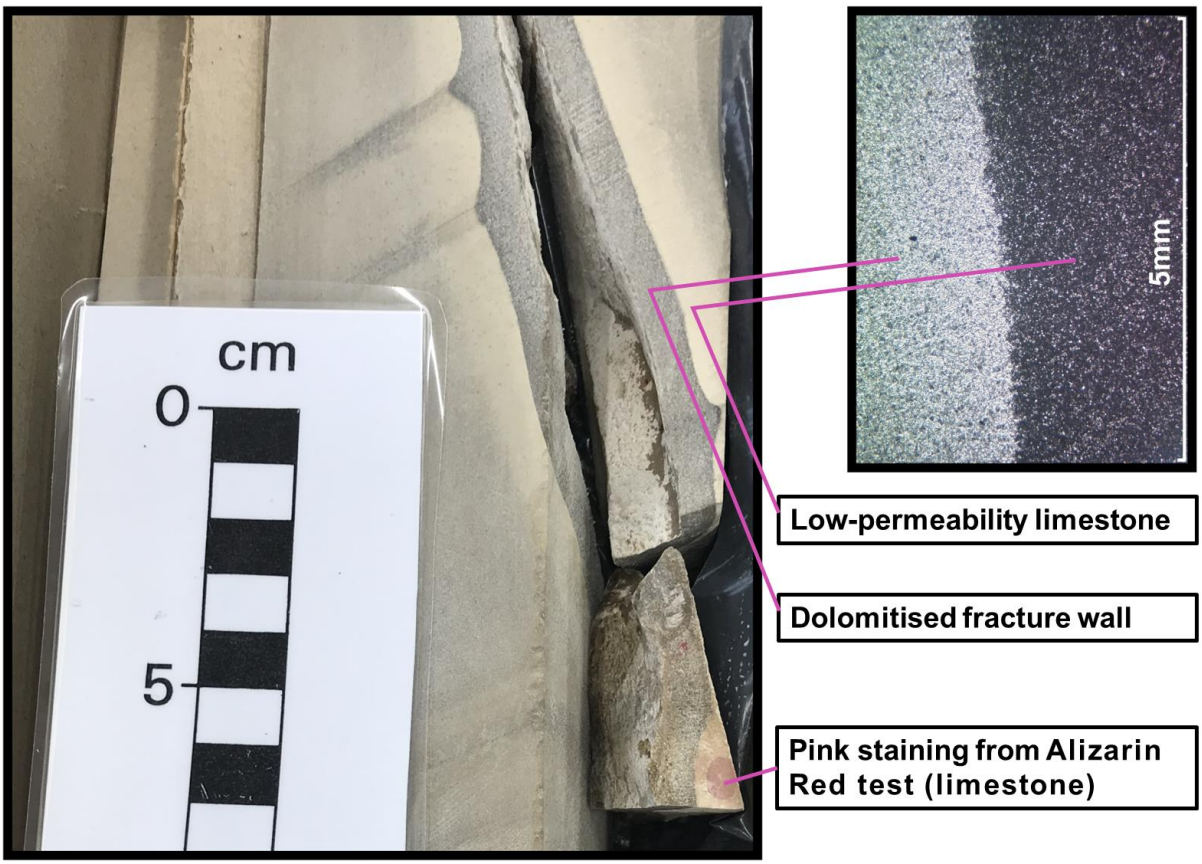

Fig. 9. *Dolomitised fracture in Z3 Plattendolomit Fm. core from well 29/27- 1.*

5.6. Implications and recommendations.

The improved understanding of the regional controls on Zechstein facies distribution could have significant implications for oil and gas exploration and energy transition research (such as seal heterogeneity and integrity which is crucial for successful carbon capture and storage). This work also provides updated understanding for other studies in restricted and semi-restricted evaporite basins.

- The evidence for sea-level rise should guarantee a Z3 and Z4 halite caprock for any Z2 Hauptdolomit Fm. platform or buildup hydrocarbon prospect, even if there is an absence of Z2 Stassfurt Halite Fm. above the target (ensuring a viable reservoir-seal pair).

- As shown by Garland et al. (2023), the Z2 basal potash can have a profound influence on seismic geometry. Along the northern margin of the Southern Zechstein Basin, the precipitation of potash salts can mimic an exaggerated Z2 Hauptdolomit Fm. shelf margin. As consistent precipitation conditions are evident in the Northern Zechstein Basin, any potential Z2 drilling targets could be influenced by this same phenomenon.
- Potential salt cavern development prospects should continue to target the homogeneous Z2 Stassfurt Halite Fm. in the Southern Zechstein Basin; however, this formation should be avoided in the Northern Zechstein Basin due to limited halite volumes and heterogeneity. Brackenridge et al. (2023) analysed the suitability of the Forth Approaches Basin for cavern development. They find that only the Z3 Leine Halite Fm. and Z4 Aller Halite Fm. demonstrate suitable evaporite thicknesses for cavern development. Whilst our study provided no concrete assessment of halite purity, the results allow for a tentative extension of this assessment across the entire western region of the Northern Zechstein Basin. Having said this, the petrophysical data presented in this study suggests that halite found elsewhere in the Northern Zechstein Basin could be far purer than that of the Forth Approaches Basin which creates opportunities for further research.
- Thickness discrepancies between evaporite bodies may not always relate to their position in the carbonate-evaporite shelf model. Rather, they could correspond to marine pathways and indicate other sources of seawater replenishment. The workflow used in this study could be applied to other marine connections in semi-restricted basins that lack detailed seismic data.

- Reflooding events in semi-restricted basins are often very sudden which can result in an absence of the transgressive systems tract. Hence, roof anhydrites may provide good chronostratigraphic markers for regional correlation.

6. CONCLUSION

Reinterpretation and integration of publicly available petrophysical datasets with newly acquired seismic data has verified the existence of a marine seaway (Jenyon's Channel) which connected the Northern and Southern Zechstein Basins and influenced Zechstein facies distribution. Whilst great volumes of Z2 halite reside within the Southern Zechstein Basin, results show that this facies remains limited within the Northern Zechstein Basin.

A thin water column submerged the MNSH structure during the Z2 sea-level highstand. During the subsequent Z2 lowstand, the only marine connection between the Northern and Southern Zechstein Basins was the narrow MNSH Seaway which acted as a gateway to the south. Although very restrictive, it did allow sufficient replenishment of seawater to provide the source of sodium chloride required to precipitate the vast Z2 halite deposits found in the Southern Zechstein Basin. The Northern Zechstein Basin remained connected to the normal salinity of the Boreal Seaway, and hence marine replenishment limited the precipitation of the Z2 halite found there.

The results highlight how this marine connection and relative sea-level rise halted the deposition of early Zechstein carbonate platforms (such as the highly prospective Orchard Platform) and left them entombed in Z3 and Z4 halite.

As such, understanding the true nature of this marine connection is important for MNSH hydrocarbon exploration especially if future efforts look to expand the Hauptdolomit play into the northern reaches of the MNSH carbonate platform based on successful analogues to the south. Similarly, a regional understanding of the controls on Zechstein salt will be important for the development of subsurface storage sites in salt caverns. Ultimately, the workflow used in this study could aid future investigations of marine gateways in semi-restricted basins that have limited seismic coverage.

7. ACKNOWLEDGEMENTS

The work contained in this publication was conducted during a PhD study undertaken as part of the Centre for Doctoral Training (CDT) in Geoscience and the Low Carbon Energy Transition and is fully funded by NeoEnergy Upstream whose support is gratefully acknowledged. The interpretations and analyses were undertaken in the Centre for Energy Transition at the University of Aberdeen, the underpinning financial and computer support for which is gratefully acknowledged. We thank the British Geological Survey and the North Sea Transition Authority for access to and permission to publish examples from their proprietary data on which these interpretations and analyses are made and we are grateful to SLB for providing academic licences for their Petrel software which was used to visualise and interrogate the seismic and petrophysical data. Proof-reading assistance from Baylee Schütte and Heather Kennedy and excellent technical discussions with Rifky Wijanarko are gratefully acknowledged. Finally, the authors thank the reviewers and editor whose feedback and comments greatly improved the manuscript

8. DATA AVAILABILITY

The seismic and petrophysical datasets related to this article can be found in the National Data Repository (NDR) and is available at [https://ndr.nstauthority.co.uk/], an open-source online data repository hosted by the North Sea Transition Authority. Similarly, the surfaces and maps of the Zechstein related to this article are available on the North Sea Transition Authority Data Centre (Brackenridge et al., 2018). The core datasets related to this article are part of the British Geological Survey's National Geological Repository and can be viewed at the core store at BGS Keyworth.

9. REFERENCES

Amiri-Garroussi, K., Taylor, J. C. M. (1992). Displaced carbonates in the Zechstein of the UK North Sea. Marine and Petroleum Geology. 9, 186-196. https://doi.org/10.1016/0264-8172(92)90090-2

Bailey, J. B., Arbin, P., Daffinoti, O., Gibson, P., Ritchie, J. S. (1993). Permo-Carboniferous plays of the Silver Pit Basin. Petroleum Geology Conference Proceedings. 4, 707-715. https://doi.org/10.1144/0040707

Brackenridge, R. E., Underhill, J. R., Jamieson, R. (2018). The Mid North Sea High: Controls on Structure, Stratigraphy and Prospectivity. Technical report and supporting documentation released via the Oil and Gas Authority Data Centre. Oil and Gas Authority, London.

Brackenridge, R. E., Underhill, J. R., Jamieson, R., Bell, A. (2020). Structural and stratigraphic evolution of the Mid North Sea High region of the UK Continental Shelf. Petroleum Geoscience. 26, 154-173. https://doi.org/10.1144/petgeo2019-076

Brackenridge, R. E., Russell, L. J., Hartley, A. J., Watson, D., & Houghton, T. D. (2023). Late Permian evaporite facies variation in the Forth Approaches Basin, North Sea: implications for hydrogen storage. Geoenergy. 1, 1-16. https://doi.org/10.1144/geoenergy2023-008

Browning-Stamp, P., Caldarelli, C., Heard, G., Ryan, J., & Hendry, J. (2023). The Zechstein Z2 Hauptdolomit platform in the southern UK Mid North Sea High and its associated petroleum plays, potential and prospectivity. Journal of Petroleum Geology. 46(3), 295-328. https://doi.org/10.1111/jpg.12840

Cheng, H., Hai, Q., Li, J., Song, J., & Ma, X. (2019). The Sensitivity of Temperature to Tachyhydrite Formation: Evidence from Evaporation

Experiments of Simulated Brines Based on Compositions of Fluid Inclusions in Halite. Geofluids. 2019, 16 pages. https://doi.org/10.1155/2019/7808036

Corfield, S. M., Gawthorpe, R. L., Gage, M., Fraser, A. J., & Besly, B. M. (1996). Inversion tectonics of the Variscan foreland of the British Isles. Journal of the Geological Society, London. 153, 17-32. https://doi.org/10.1144/gsjgs.153.1.001

Coward, M. P. (1995). Structural and tectonic setting of Permo-Triassic basins of northwest Europe. Geological Society of London Special Publication. 91, 7-39. https://doi.org/10.1144/GSL.SP.1995.091.01.02

Clark, D. N. (1986). The Distribution of Porosity in Zechstein Carbonates. Geological Society of London Special Publication. 23, 121-149. https://doi.org/10.1144/GSL.SP.1986.023.01.09

Day, G. A., Cooper, B. A., Anderson, C., Burgers, W. F. J., Ronnevik, H. C., Schoneich, H. (1981). Regional seismic structure maps of the North Sea. Petroleum geology of the continental shelf of north-west Europe. Heyden & Son Ltd: Institute of Petroleum, London.

Doornenbal, J. C., and A. G. Stevenson (2010), Geological Atlas of the Southern Permian Basin Area: Houten, the Netherlands, European Association of Geoscientists and Engineers Publications.

Donato, J. A., Martindale, W., & Tully, M. C. (1983). Buried granites within the Mid North Sea High. Journal of the Geological Society. 140, 825-837. https://doi.org/10.1144/gsjgs.140.5.0825

Fluteau, F., Besse, J., Broutin, J., & Ramstein, G. (2001). The Late Permian climate. What can be inferred from climate modelling concerning Pangea scenarios and Hercynian range altitude? Palaeogeography, Palaeoclimatology, Palaeoecology. 167(1-2), 39-71. https://doi.org/10.1016/S0031-0182(00)00230-3

Garland, J., Tiltman, C., Inglis, C. (2023). Sedimentology, palaeogeography and diagenesis of the upper Permian (Z2) Hauptdolomit Formation on the southern margin of the Mid North Sea High and implications for reservoir prospectivity. Journal of Petroleum Geology. 46(3), 329-360. https://doi.org/10.1111/jpg.12841

Glennie, K. W. (1995). Permian and Triassic rifting in northwest Europe. Geological Society of London Special Publication. 91, 1-5. https://doi.org/10.1144/GSL.SP.1995.091.01.01

Glennie, K. W.& Underhill, J. R. (1998). Origin, Development and Evolution of Structural Styles. Petroleum Geology of the North Sea: Basic Concepts and Recent Advances. https://doi.org/10.1002/9781444313413.ch2

Grant, R. J., Underhill, J. R., Hernández-Casado, J., Barker, S. M., & Jamieson, R. J. (2019). Upper Permian Zechstein Supergroup carbonate-evaporite platform palaeomorphology in the UK Southern North Sea. Marine and Petroleum Geology. 100, 484-518. https://doi.org/10.1016/j.marpetgeo.2017.11.029

Habicht, J. K. A. (1979). Paleoclimate, paleomagnetism, and continental drift. AAPG Studies in Petroleum Geology No. 9. The American Association of Petroleum Geologists, Tulsa, Oklahoma, 74101, USA.

Heeremans, M., Timmerman, M. J., Kirstein, L. A., & Faleide, J. I. (2004). New constraints on the timing of late Carboniferous-early Permian volcanism in the central North Sea. Geological Society of London Special Publication. 223, 177-193. https://doi.org/10.1144/GSL.SP.2004.223.01.08

Jackson, C. A.-L., & Stewart, S. A. (2017). Chapter 8 - Composition, Tectonics, and Hydrocarbon Significance of Zechstein Supergroup Salt on the United Kingdom and Norwegian Continental Shelves. Permo-Triassic Salt Provinces of Europe, North Africa and the Atlantic Margins: Tectonics and Hydrocarbon Potential. 175-201. https://doi.org/10.1016/b978-0-12-809417-4.00009-4

Jenyon, M. K., Cresswell, P. M., & Taylor, J. C. M. (1984). Nature of the connection between the Northern and Southern Zechstein Basins across the Mid North Sea High. Marine and Petroleum Geology. 1(4), 355-363. https://doi.org/10.1016/0264-8172(84)90136-3

Jenyon, M. K. (1987). Re-entrants of Zechstein Z2 salt in the Mid North Sea High. Marine and Petroleum Geology. 5(4), 352-358. https://doi.org/10.1016/0264-8172(88)90028-1

Jenyon, M. K. & Taylor, J. C. (1988). Dissolution effects and reef-like features in the Zechstein across the Mid North Sea High. The Zechstein Facies in Europe, Springer-Verlag, Berlin. 51-75.

Johnson, H., Warrington, G., Stoker, S. J. (1994). 6. Permian and Triassic of the Southern North Sea. Lithostratigraphic Nomenclature of the UK North Sea, vol. 6 British Geological Survey, Nottingham

Kroner, U., & Romer, R. L. (2013). Two plates - Many subduction zones: The Variscan orogeny reconsidered. Gondwana Research. 24(1), 298–329. https://doi.org/10.1016/j.gr.2013.03.001

Lukanin, O. A. (2016). Chlorine partitioning between melt and aqueous chloride fluid phase during granite magma degassing. Part II. Crystallization-induced degassing of melts. Geochemistry International. 54, 660–680. https://doi.org/10.1134/S0016702916080061

Marín, D., Cardozo, N., & Escalona, A. (2023). Compositional variation of the Zechstein Group in the Norwegian North Sea: Implications for underground storage in salt caverns. Basin Research. 35(4), 1460-1485. https://doi.org/10.1111/bre.12761

McCann, T., Pascal, C., Timmerman, M. J., Krzywiec, P., López-Gómez, J., Wetzel, A., Krawczyk, C. M., Rieke, H., & Lamarche, J. (2006). Post-Variscan (end Carboniferous-Early Permian) basin evolution in Western and Central Europe. Geological Society Memoir. 32, 355-388). https://doi.org/10.1144/GSL.MEM.2006.032.01.22

McKie, T. (2017). Paleogeographic Evolution of Latest Permian and Triassic Salt Basins in Northwest Europe. Permo-Triassic Salt Provinces of Europe,

North Africa and the Atlantic Margins: Tectonics and Hydrocarbon Potential. 159–173. https://doi.org/10.1016/B978-0-12-809417-4.00008-2

Muhammed, N. S., Haq, B., al Shehri, D., Al-Ahmed, A., Rahman, M. M., & Zaman, E. (2022). A review on underground hydrogen storage: Insight into geological sites, influencing factors and future outlook. Energy Reports. 8, 461-499. https://doi.org/10.1016/j.egyr.2021.12.002

Mulholland, P., Esestime, P., Rodriguez, K., & John Hargreaves, P. (2018). The role of palaeorelief in the control of Permian facies distribution over the Mid North Sea High, UK Continental Shelf. Geological Society Special Publication. 471, 155-175. https://doi.org/10.1144/SP471.8

Nance, R. D., Gutiérrez-Alonso, G., Keppie, J. D., Linnemann, U., Murphy, J. B., Quesada, C., Strachan, R. A., & Woodcock, N. H. (2009). Evolution of the Rheic Ocean. Gondwana Research. 17(2-3), 194-222. https://doi.org/10.1016/j.gr.2009.08.001

Patruno, S., Kombrink, H., & Archer, S. G. (2022). Cross-border stratigraphy of the Northern, Central and Southern North Sea: a comparative tectono-stratigraphic megasequence synthesis. Geological Society of London Special Publication. 494, 13–83. http://doi.org/10.1144/SP494-2020-228

Patruno, S., Reid, W., Jackson, C. A. L., & Davies, C. (2017). New insights into the unexploited reservoir potential of the Mid North Sea High (UKCS quadrants 35-38 and 41-43): A newly described intra-Zechstein sulphate-carbonate platform complex. Petroleum Geology Conference Proceedings. 8, 87-124. https://doi.org/10.1144/PGC8.9

Peryt, T. M., Raczyński, P., Peryt, D., & Chłódek, K. (2012). Upper Permian reef complex the basal facies of the Zechstein Limestone (Ca1), western Poland. Geological Journal. 47(5), 537-552. https://doi.org/10.1002/gj.2440

Rider, M. and Kennedy, M. (2002) The geological interpretation of well logs. Sutherland: Rider-French Consulting.

Rossi, V. M., Longhitano, S. G., Olariu, C., Chiocci, F. L. (2023). Straits and seaways: controls, processes and implications in modern and ancient systems. Geological Society Special Publication. 523, 1-15. https://doi.org/10.1144/SP523-2022-271

SaltWorkConsultants. (2023). Wireline-skills-evaporite. Available at: https://saltworkconsultants.com/wireline-skills-evaporite/ (Accessed: 02 August 2023).

Sarg, J. F. (2001). The sequence stratigraphy, sedimentology, and economic importance of evaporite-carbonate transitions: a review. Sedimentary Geology. 140(1-2), 9-34. https://doi.org/10.1016/S0037-0738(00)00170-6

Schulmann, K., Catalán, J. R. M., Lardeaux, J. M., Janoušek, V., & Oggiano, G. (2014). The Variscan orogeny: Extent, timescale and the formation of the European crust. Geological Society of London Special Publication. 405, 1-6. https://doi.org/10.1144/SP405.15

Sørensen, A. M., Håkansson, E., & Stemmerik, L. (2007). Faunal migration into the Late Permian Zechstein Basin - Evidence from bryozoan

palaeobiogeography. Palaeogeography, Palaeoclimatology, Palaeoecology. 251(2), 198-209. https://doi.org/10.1016/j.palaeo.2007.03.045

Smith, D. B. (1979). Rapid marine transgressions and regressions of the Upper Permian Zechstein Sea. Journal of the Geological Society. 136, 155-156. https://doi.org/10.1144/gsjgs.136.2.0155

Smith, D. B., & Taylor, J. C. M. (1989). A “North-west Passage” to the southern Zechstein Basin of the UK North Sea. Proceedings of the Yorkshire Geological Society. 47, 313-320. https://doi.org/10.1144/pygs.47.4.313

Taylor, (1993). Pseudo-reefs beneath Zechstein salt on the northern flank of the Mid North Sea High. Petroleum Geology Conference Proceedings. 4, 749-757. https://doi.org/10.1144/0040749

Trewin, N. H., Bramwell, M., G. (1991). The Auk Field, Block 30/16, UK North Sea. Geological Society Memoir. 14, 227-236. https://doi.org/10.1144/GSL.MEM.1991.014.01.28

Tucker, M. E. (1991). Sequence stratigraphy of carbonate-evaporite basins: Models and application to the Upper Permian (Zechstein) of northeast England and adjoining North Sea. Journal of the Geological Society. 148(4), 1019-1036. https://doi.org/10.1144/gsjgs.148.6.1019

Underhill, J. R., & Hunter, K. L. (2008). Effect of Zechstein Supergroup (Z1 cycle) Werrahalit pods on prospectivity in the southern North Sea. American Association of Petroleum Geologists Bulletin. 92, 827-851. https://doi.org/10.1306/02270807064

Underhill, J. R., & Richardson, N. (2022). Geological controls on petroleum plays and future opportunities in the North Sea Rift Super Basin. American Association of Petroleum Geologists Bulletin. 106(3), 573-631. https://doi.org/10.1306/07132120084

Underhill, J. R., de Jonge-Anderson, I., Hollingsworth, A. D., Fyfe, L. C. (2023). Use of exploration methods to repurpose and extend the life of a super basin as a carbon storage hub for the energy transition. American Association of Petroleum Geologists Bulletin. 107(8), 1419-1474. https://doi.org/10.1306/04042322097

Van den Belt, F. J. G., & de Boer, P. L. (2007). A shallow-basin model for “saline giants” based on isostasy-driven subsidence. Sedimentary Processes, Environments and Basins: A Tribute to Peter Friend. https://doi.org/10.1002/9781444304411.ch11

Van Wees, J.-D., Stephenson, R. A., Ziegler, P. A., Bayer, U., Mccann, T., Dadlez, R., Gaupp, R., Narkiewicz, M., Bitzer, F., & Scheck, M. (2000). On the origin of the Southern Permian Basin, Central Europe. Marine and Petroleum Geology. 17(1), 43-59. https://doi.org/10.1016/S0264-8172(99)00052-5

Warren, J. K. (2016). Evaporites a geological compendium. Springer International Publishing.

Warren, J. K. (2017). Calcium Chloride (CaCl2) Article 2 of 2: CaCl2 minerals across time and space. Salty Matters. Available at:

https://www.saltworkconsultants.com/downloads/27.%20CaCl2%20brines%202%20of%202.pdf

Ziegler, P. A. (1975). Geologic Evolution of North Sea and Its Tectonic Framework. American Association of Petroleum Geologists Bulletin. 59, 1073-1097. https://doi.org/10.1306/83D91F2E-16C7-11D7-8645000102C1865D

Ziegler, P. A. (1992). North Sea rift system. Tectonophysics. 208(1-3), 55-75. https://doi.org/10.1016/0040-1951(92)90336-5

Ziegler, P. A. (1988). Chapter 30 - Post-Hercynian plate reorganization in the Tethys and Arctic - North Atlantic domains. Developments in Geotectonics. 22, 711-755. https://doi.org/10.1016/B978-0-444-42903-2.50035-X